Pergamon

Geochimica et Cosmochimica Acta, Vol. 67, No. 11, pp. 2005–2025, 2003

0016-7037/03 $30.00 + .00

PII S0016-7037(02)01116-X

Sr, C, and O isotope geochemistry of Ordovician brachiopods: A major isotopic event around the Middle-Late Ordovician transition

GRAHAM A. SHIELDS,[1,*†] GILES A. F. CARDEN,[2‡] JAN VEIZER,[1,3] TÕNU MEIDLA,[4] JIA-YU RONG,[5] and RONG-YU LI[6]

[1]Ottawa-Carleton Geoscience Centre, University of Ottawa, Ottawa, ON, K1N 6N5, Canada
[2]Formerly Institut für Geologie, Mineralogie und Geophysik, Ruhr Universität, 44780 Bochum, Germany
[3]Institut für Geologie, Mineralogie und Geophysik, Ruhr Universität, 44780 Bochum, Germany
[4]Institute of Geology, Tartu University, 46 Vanemuise Street, 51014 Tartu, Estonia
[5]Nanjing Institute of Geology and Palaeontology, Chinese Academy, Nanjing, 210008, Jiangsu, China
[6]Department of Earth and Atmospheric Sciences, University of Alberta, Edmonton, AB, T6G 2E3, Canada

(*Received September* 6, 2001; *accepted in revised form July* 29, 2002)

Abstract—Here we present Sr, C, and O isotope curves for Ordovician marine calcite based on analyses of 206 calcitic brachiopods from 10 localities worldwide. These are the first Ordovician-wide isotope curves that can be placed within the newly emerging global biostratigraphic framework. A total of 182 brachiopods were selected for C and O isotope analysis, and 122 were selected for Sr isotope analysis. Seawater $^{87}Sr/^{86}Sr$ decreased from 0.7090 to 0.7078 during the Ordovician, with a major, quite rapid fall around the Middle–Late Ordovician transition, most probably caused by a combination of low continental erosion rates and increased submarine hydrothermal exchange rates. Mean $\delta^{18}O$ values increase from −10‰ to −3‰ through the Ordovician with an additional short-lived increase of 2 to 3‰ during the latest Ordovician due to glaciation. Although diagenetic alteration may have lowered $\delta^{18}O$ in some samples, particularly those from the Lower Ordovician, maximum $\delta^{18}O$ values, which are less likely to be altered, increase by more than 3‰ through the Ordovician in both our data and literature data. We consider that this long-term rise in calcite $\delta^{18}O$ records the effect of decreasing tropical seawater temperatures across the Middle–Late Ordovician transition superimposed on seawater $\delta^{18}O$ that was steadily increasing from ≤ -3‰ standard mean ocean water (SMOW). By contrast, $\delta^{13}C$ variation seems to have been relatively modest during most of the Ordovician with the exception of the globally documented, but short-lived, latest Ordovician $\delta^{13}C$ excursion up to +7‰. Nevertheless, an underlying trend in mean $\delta^{13}C$ can be discerned, changing from moderately negative values in the Early Ordovician to moderately positive values by the latest Ordovician. These new isotopic data confirm a major reorganization of ocean chemistry and the surface environment around 465 to 455 Ma. The juxtaposition of the greatest recorded swings in Phanerozoic seawater $^{87}Sr/^{86}Sr$ and $\delta^{18}O$ at the same time as one of the largest marine transgressions in Phanerozoic Earth history suggests a causal link between tectonic and climatic change, and emphasizes an endogenic control on the O isotope budget during the Early Paleozoic. Better isotopic and biostratigraphic constraints are still required if we are to understand the true significance of these changes. We recommend that future work on Ordovician isotope stratigraphy focus on this outstanding Middle–Late Ordovician event.

1. INTRODUCTION

Isotope stratigraphy has come a long way since its early days. Initial expectations of theoretically predictable trends through time (Wickman, 1948; Clayton and Degens, 1959) were quashed during the 1960s and 1970s (Peterman et al., 1970), and over the last 30 years or so researchers have established isotopic trends of successively increasing complexity and sophistication (Veizer et al., 1980; Burke et al., 1982; Smalley et al., 1994; Veizer et al., 2000). The resultant isotope curves can be used for stratigraphic correlation as well as for tracing geological processes, a dual application that makes them a particularly attractive research aim. Sr and C isotopes have proved especially popular in both regards and are the mainstays of modern chemostratigraphy (Veizer et al., 1999).

The Ordovician period has been the subject of several isotope stratigraphy studies, although few have attempted to cover the entire Ordovician (Veizer et al., 1986; Wadleigh and Veizer, 1992; Qing et al., 1998) and fewer still can be incorporated within a globally sound biostratigraphic framework. The present study brings together biostratigraphically constrained Sr, C, and O isotope data for biogenic marine calcite covering the entire Ordovician period. It is hoped that this study will serve as a foundation for future isotope studies, while helping to constrain further the relative timing and rates of isotopic and geological events during the Ordovician Period. In accordance with the current state-of-the-art, this study reports the Sr, C, and O isotope compositions of low-Mg calcite brachiopods after diagenetic screening for good preservation.

2. GLOBAL ORDOVICIAN BIOSTRATIGRAPHY

One major challenge facing Paleozoic isotope stratigraphers involves biostratigraphic correlation. Although biostratigraphy is the only stratigraphic correlation tool that enables the reconstruction of globally significant isotope curves for Paleozoic time, age uncertainty caused by insufficient biostratigraphic

* Author to whom correspondence should be addressed (graham.shields@jcu.edu.au).
† *Present address:* School of Earth Sciences, James Cook University, Townsville, Queensland 4811, Australia.
‡ *Present address:* Research and Development Services Office, Senate House, University of Warwick, Coventry CV4 7AL, United Kingdom.

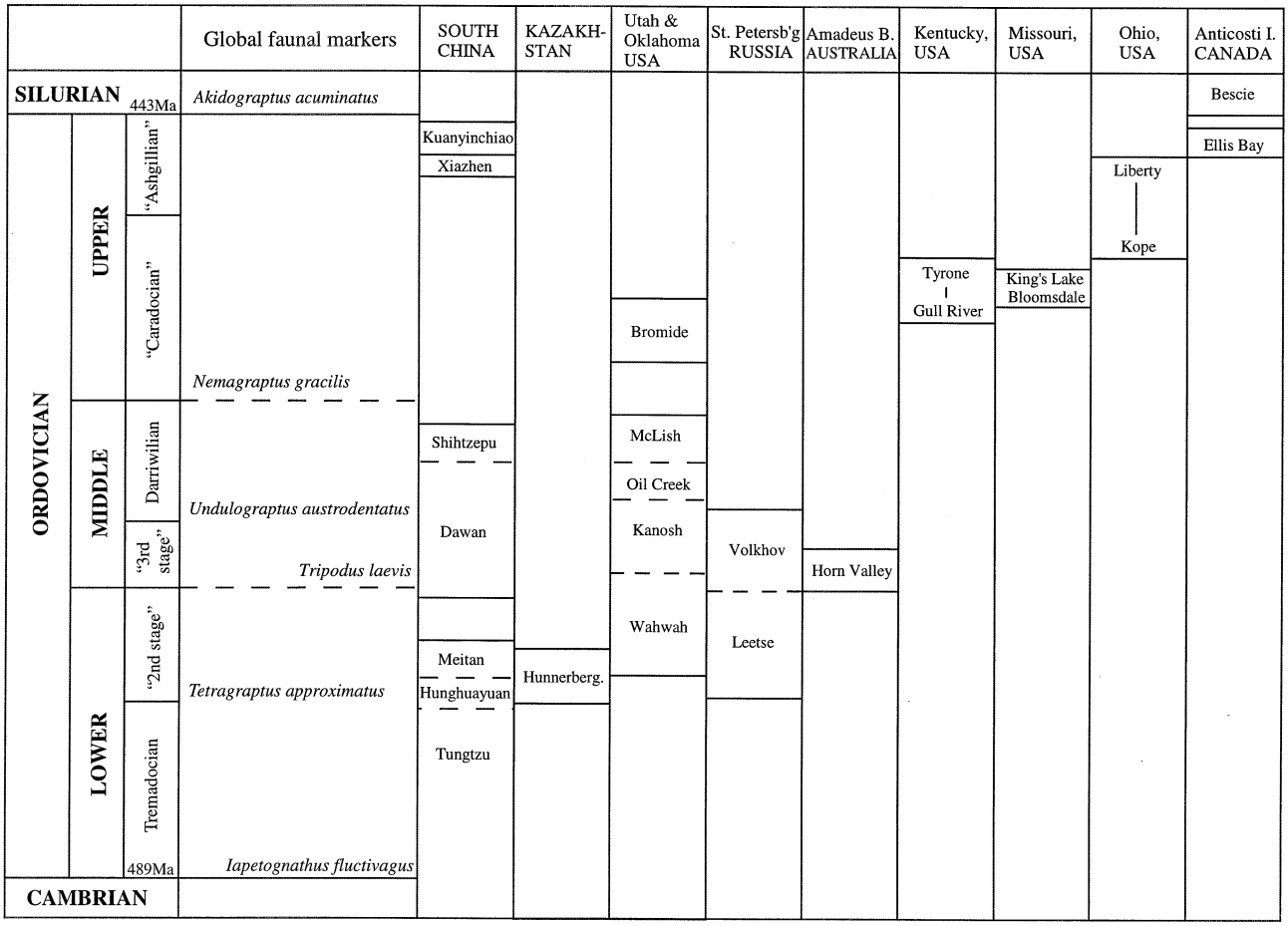

Fig. 1. Nomenclature and correlation of Ordovician stratigraphic units for the studied sections. For age assignments see text.

resolution is often the major source of error in isotope curves (Veizer et al., 1997). The Ordovician period, in particular, suffers from the lack of a coherent global biostratigraphic framework, which renders many previous isotope studies exceedingly difficult to assess in global terms. Despite the widespread use of the British stratigraphic nomenclature in the geological literature, the widely known stratigraphic divisions of the British Ordovician (Tremadoc, Arenig, Llanvirn, Llandeilo, Caradoc, and Ashgill) have not been generally accepted outside the British Isles (Webby, 1998) and are currently being radically overhauled in their places of origin (Fortey et al., 1995). To overcome this problem, attempts are under way to establish a global biostratigraphic framework for the Ordovician, into which geological and geochemical data can be placed. This work is part of the mandate of the currently active International Geological Correlation Programme (IGCP) Project 410: "Ordovician biodiversity." We attempt here to incorporate our isotope data into the newly emerging global biostratigraphic framework (Webby, 1998).

In this article, we acknowledge the latest guidelines and decisions of the International Commission on Stratigraphy (ICS) as outlined in Webby (1998) and more recent bulletins of the ICS. Consequently, we recognize the subdivision of the Ordovician System into three global series: Lower, Middle, and Upper, the time equivalents of which are currently estimated to be of unequal duration, being 18, 11.5, and 16.5 Ma, respectively, although there is still considerable uncertainty on this point. Each global series is to be divided into two global stages, only two of which have been named officially, these being the Tremadocian and Darriwilian stages, which are the first and fourth stages, respectively. The remaining four stages have not yet been named or defined officially and are shown in the text in inverted commas, e.g., "2nd stage" and "3rd stage" (Fig. 1). Because there is no formally defined boundary dividing the upper series, we use the terms "Caradocian" and "Ashgillian" until such time as these are formally defined. To incorporate our data into these global series and stages, they have been assigned to global time slices, 19 in total, using the current biostratigraphic guidelines set out in the forthcoming book *The Great Ordovician Biodiversification Event*, edited by B. Webby and M. Droser (Webby, personal communication). We do not report data for all of these time-slices, and this inadequacy should be addressed by future studies, especially on Lower Ordovician successions.

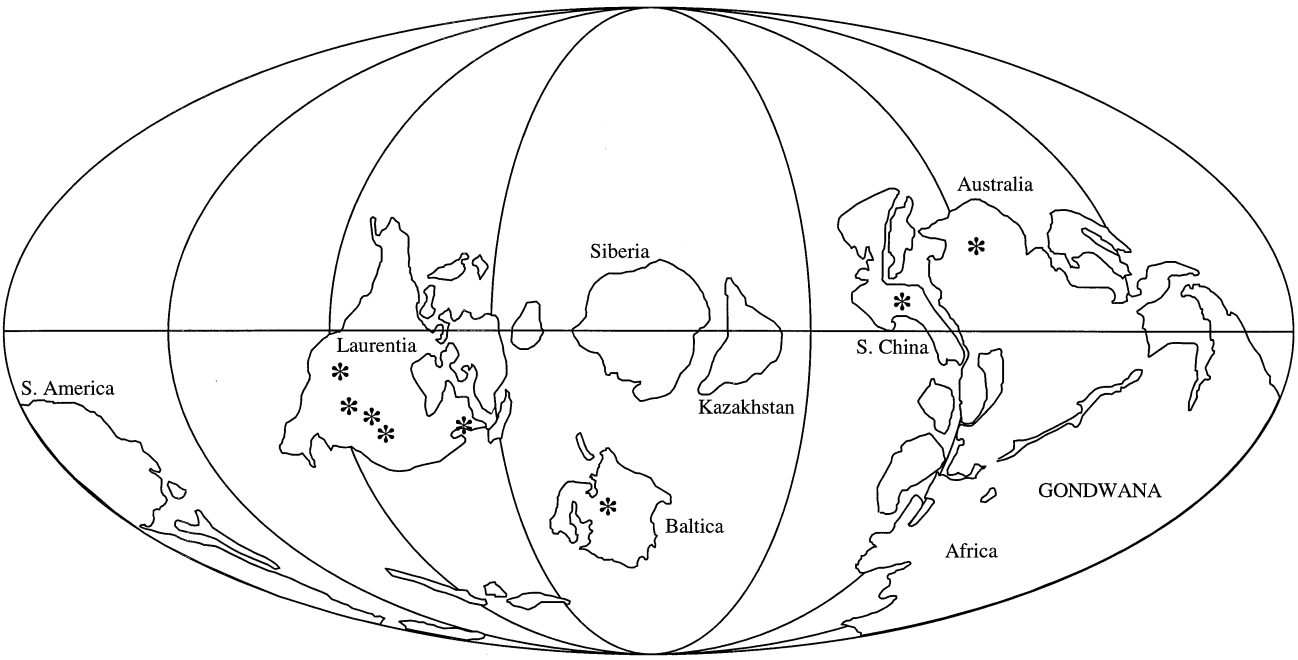

Fig. 2. Paleogeographic reconstruction of the Early Ordovician (after Scotese and McKerrow, 1991) with section locations marked by asterisks.

3. SAMPLING LOCALITIES

Samples were collected from almost the entire Ordovician (Fig. 1) with 10 locations on four continents (Fig. 2): Utah, USA; Cincinnati, Ohio, USA; Lexington, Kentucky, USA; St. Louis, Missouri, USA; Arbuckle Mountains, Oklahoma, USA; St. Petersburg, Russia; southern Urals, Kazakhstan; South China; Amadeus Basin, Australia; Anticosti Island, Québec, Canada. All represent low paleolatitude marine basins between 30°N and 30°S, with the exception of Baltica (St. Petersburg, Russia), which was possibly further south (30°S – 60°S) during the Early and Middle Ordovician (Scotese and McKerrow, 1991).

4. METHODOLOGY

Where possible, whole brachiopods or otherwise shell fragments were collected. Shells were either completely articulated, single valves, or fragments, which were either embedded in their limestone matrix or had worked themselves free of the host rock. In most instances some sediment adhered to the shell, particularly in the sulci between strong ribs. This was removed using a mounted stainless steel needle and a surgical scalpel blade. The outer abraded secondary lamella shell layer was then picked off using a mounted needle. The primary layer, which is more frequently diagenetically altered (Carpenter and Lohmann, 1995), was rarely observed. This revealed the entirely clean inner shell layers, which are normally pearlescent cream or white in color. It has been demonstrated that calcite from the hinge, brachidium, foramen, interarea, and muscle scars of modern brachiopod shells tend to be abnormally depleted in both ^{18}O and ^{13}C (Carpenter and Lohmann, 1995). Therefore, these areas were avoided during shell sampling. Shell fragments were then placed in an ultrasonic bath filled with deionized water to remove any remaining extraneous material. Further details of sampling techniques and selection criteria are reported in Azmy et al. (1998) and Veizer et al. (1999). Two shell portions were subsequently picked for stable isotope and trace element analyses, and strontium isotope analyses, respectively. Where possible, remaining portions were retained for examination using cathodoluminescence and scanning electron microscopy (SEM). For Ca, Mn, Fe, Sr, and Mg concentrations, 5 to 10 mg of the shell were dissolved in 10 mL of 2N HCl and analyzed using a Varian Spectra AA.300 atomic absorption spectrometer. For stable isotopes, 1 to 5 mg of powdered brachiopod shell was reacted in 100% orthophosphoric acid offline at 50°C and analyzed using a Finnigan MAT 251 mass spectrometer. Analytical reproducibility for both O and C isotopes was within 0.1‰. Sr isotope analysis was carried out on 0.5 to 2 mg of sample after dissolution in 2.5N HCl. Sr was concentrated using Rad AG50WX8 ion-exchange resin and eluted with 2.5N HCl. After evaporation of the eluant, approximately 150 to 250 ng Sr was loaded on single Re filaments using a Ta_20_5-HNO_3-HF-H_3PO_4 solution (Birck, 1986) and analyzed using a Finnigan MAT 262 mass spectrometer in static mode at the Ruhr University, Bochum in Germany. International standard NBS SRM 987 yielded a ratio of 0.710231. This mean value represents the average ratio over 4 ½ years and 550 measurements and bears a standard deviation (1 SD) of 38×10^{-6}, and standard error of 17×10^{-7}. Further details of standard normalization are given in Diener et al. (1996).

5. RESULTS

5.1. Shell Microstructure

Representative samples from all brachiopod sample suites were investigated using SEM, some results of which are repro-

duced in Figure 3. Well-preserved secondary shell layers ought to retain a series of lamellar, stacked calcite rods or crystallites with no evidence for dissolution or reprecipitation (Popp et al., 1986). Brachiopods from this study reveal generally good textural preservation of this secondary layer, although microdissolution vugs are present in some samples (KY12 to 15, Alb01, Alb06b). Recrystallization appears to have been minor in most cases, and, where present, is comparable to that from a study carried out previously by G.C. of uppermost Ordovician brachiopods from Estonia and Canada (Carden, 1995).

5.2. Trace Elements and Chemical Preservation of the Brachiopods

Comparison between the trace element contents of Ordovician brachiopods from this study and Holocene brachiopods (Fig. 4) shows that about half of our samples fall within the predicted ranges for unaltered brachiopods of Sr = 500 to 2000 ppm and Mn = <200 ppm (Morrison and Brand, 1986; Brand and Logan, personal communication, 2001). Fe and Mg concentrations (Appendix A1) are also higher in some cases than the <600 ppm and <2000 ppm, respectively, that would normally be expected for unaltered brachiopods. Consequently, our brachiopod samples from the Darriwilian and Tremadocian stages, in particular, appear to have somewhat more "altered" trace element compositions than those from previous studies that covered the Ordovician and Silurian Periods (Qing and Veizer, 1994; Azmy et al., 1998) (Fig. 4). However, at least half of our samples from each of the four other Ordovician stages have more favorable trace element compositions, while their Mn and Sr contents show no correlation that might be attributed to a diagenetic trend (Fig. 4). Although it is true that about half of our samples fall outside the preferred range for trace elements, we stress that the relationship between textural preservation of samples and trace elements (Brand and Veizer, 1980) has only a statistical validity. This is clearly documented by our brachiopod samples (Fig. 3), which fail to show any simple relationship between Sr concentration or Mn/Sr ratios and preservation of a seawater $^{87}Sr/^{86}Sr$ signature (Figs. 3 and 5).

5.3. Strontium Isotopes

All Sr isotope data are listed in Appendix A1, summarized in Table 1, and plotted in Figure 6. They are discussed in ascending stratigraphic order. *Lower Ordovician*: Mean $^{87}Sr/^{86}Sr$ ratios from the Lower Ordovician of China, Kazakhstan, and Utah, USA lie consistently around 0.7090 (n = 17). *Middle Ordovician*: $^{87}Sr/^{86}Sr$ ratios through almost the entire Middle Ordovician lie consistently between 0.70870 and 0.70890 (n = 29) with the exception of three anomalously radiogenic samples from the Lower Olive Shale, Utah and two samples from the uppermost Middle Ordovician of Oklahoma that yield significantly lower ratios of 0.70860 and 0.70865. *Upper Ordovician*: $^{87}Sr/^{86}Sr$ ratios from the Upper Ordovician are markedly less radiogenic than those of the Middle Ordovician, and reveal a restricted range averaging 0.7080 (n = 70) and consistent lowermost ratios around 0.70785.

5.4. Carbon and Oxygen Isotopes

The carbon and oxygen isotope data obtained in this study are listed in Appendix A1, summarized in Table 1, and plotted in Figure 7. They are discussed in ascending stratigraphic order. *Lower Ordovician* samples yield negative $\delta^{13}C$ between –1.2‰ and 0‰, averaging –0.9‰ (n = 15). $\delta^{18}O$ for the Lower Ordovician ranges between –11.1‰ and –8.2‰, averaging –9.3‰. *Middle Ordovician* samples reveal a wide range of $\delta^{13}C$ between –3.0‰ and +1.8‰ but are also predominantly negative, averaging –1.2‰ (n = 65), contrasting little with the Lower Ordovician. $\delta^{18}O$ for the Middle Ordovician ranges between –9.0‰ and –5.4‰, averaging –7.6‰. The *Upper Ordovician* reveals a successive rise in mean $\delta^{13}C$ from –0.7‰ (n = 14) in the lower "Caradocian" to +1.6‰ in the uppermost Ordovician (n = 31), where $\delta^{13}C$ reveals a considerable range between 0.2‰ and 5.8‰. $\delta^{18}O$ for the Upper Ordovician ranges between –6.9‰ and –3.5‰ with the exception of the uppermost Ordovician, within which interval $\delta^{18}O$ reaches exceptional values as high as +0.2‰.

6. DISCUSSION

6.1. Strontium Isotopes

Lowermost $^{87}Sr/^{86}Sr$ ratios for any particular stratigraphic level generally correspond most closely to the seawater $^{87}Sr/^{86}Sr$ value due to the tendency of diagenetic alteration to increase $^{87}Sr/^{86}Sr$ (Veizer and Compston, 1974; McArthur, 1994; Stille and Shields, 1997). This general rule-of-thumb appears to hold true for the brachiopod samples in our study, too, as all obvious outliers are more radiogenic and belong to data groups exhibiting a broad range of values that cannot possibly all represent seawater values owing to the long, Myr-scale residence time of strontium in seawater. For example, the wide range of $^{87}Sr/^{86}Sr$ data from the Lower Olive Shale, Utah must indicate that those relatively radiogenic ratios are unrepresentative of contemporary seawater. Conversely, we can be confident that datasets which exhibit a restricted range of relatively low $^{87}Sr/^{86}Sr$ ratios approximate more closely seawater $^{87}Sr/^{86}Sr$.

Our study reveals decreasing Sr isotope ratios through the Ordovician confirming several previous studies, which concluded that seawater $^{87}Sr/^{86}Sr$ decreased during the Ordovician from ~0.7090 to 0.7078 (Veizer and Compston, 1974; Burke et al., 1982; Veizer et al., 1986; Denison et al., 1998; Qing et al., 1998). This general trend is discussed in more detail below. There is a relative abundance of strontium isotope work from around the Cambrian–Ordovician boundary, which constrains seawater $^{87}Sr/^{86}Sr$ to $0.709000 \pm 50 \times 10^{-6}$ at this time (Gao and Land, 1991; Johnson and Goldstein, 1993; Qing et al., 1998; Ebneth et al., 2001). Our limited new data for the Tremadocian of South China are consistent with these results. Although mean $^{87}Sr/^{86}Sr$ reveals scant variation among our Lower Ordovician brachiopods, lowest ratios for each individual dataset (Table 1) indicate that seawater $^{87}Sr/^{86}Sr$ fell gradually from 0.7090 to 0.7088 during the Early Ordovician (cf. Qing et al., 1998). Both mean and lowest ratios are then invariant at around 0.7087 during much of the Middle Ordovician, suggesting that seawater $^{87}Sr/^{86}Sr$ did not change greatly during that time. A second, more considerable fall in

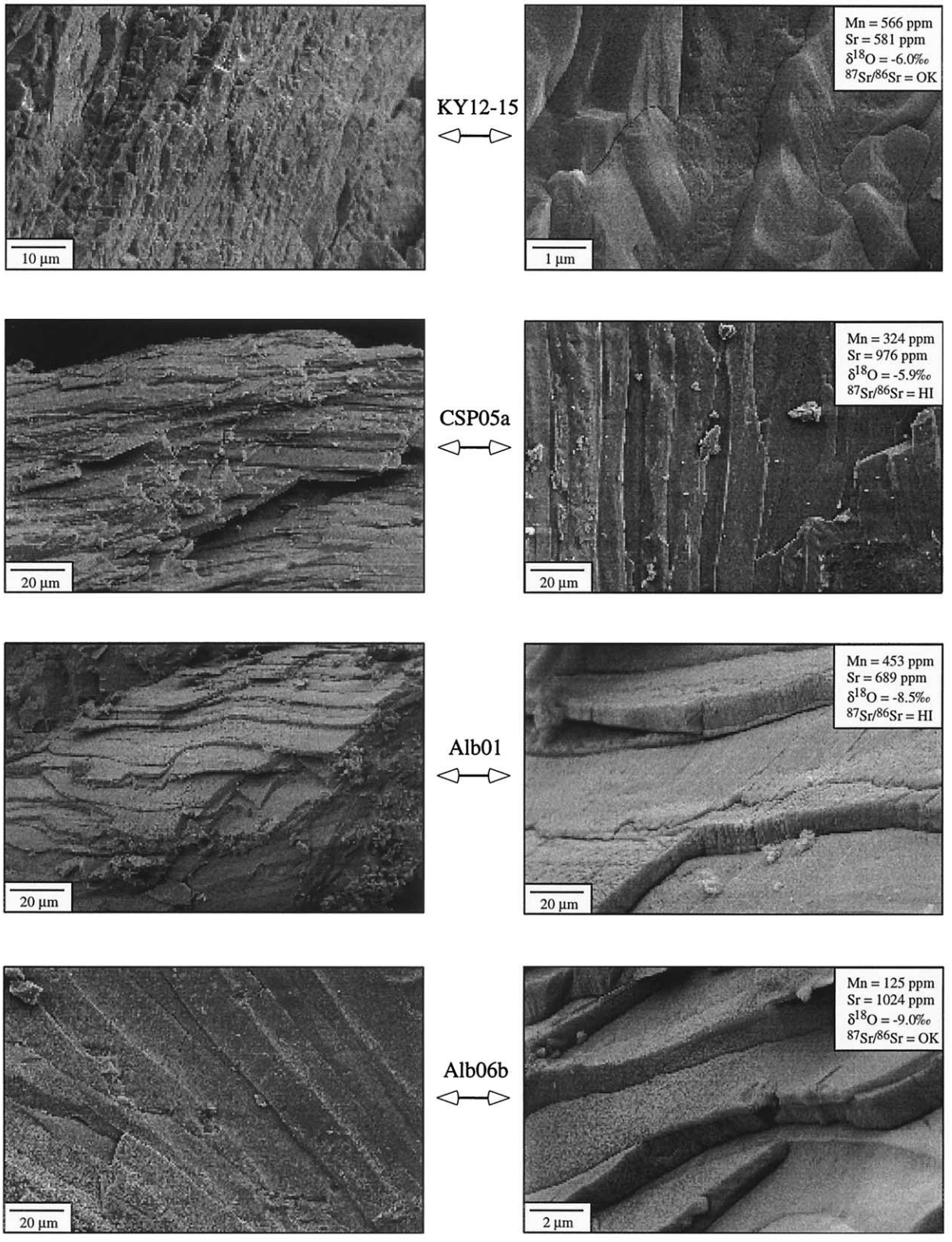

Fig. 3. SEM photomicrographs of four Ordovician brachiopods from top (youngest) to bottom (oldest): KY12 to 15 (*C. wilsoni* Zone, Upper Ordovician, Lexington Limestone, Kentucky, USA); CSP05a (*D. hirundo* Zone, Middle Ordovician, Leetse Formation, Russia); Alb01 (*D. nitidus* Zone, Lower Ordovician, Kanosh Shale, Utah, USA); Alb06b (*D. deflexus* Zone, Lower Ordovician, Simpson Group, Oklahoma, USA). Geochemical data are also given with $^{87}Sr/^{86}Sr$ ratios shown as OK and HI (apparently unaltered or somewhat radiogenic, respectively). Note that there is no apparent correlation between degree of diagenetic alteration (microstructure, Mn/Sr, $^{87}Sr/^{86}Sr$) and $\delta^{18}O$.

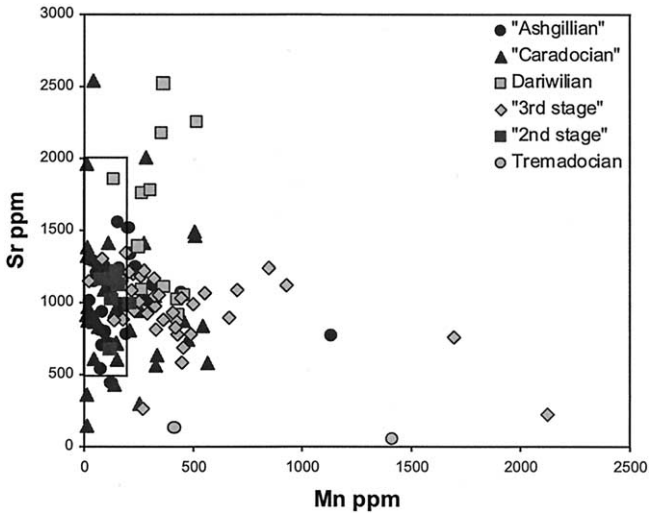

Fig. 4. Scatter diagram of Sr vs. Mn content in Ordovician brachiopod shells. The box represents the expected range for Holocene brachiopods based on data from Lowenstam (1961), Dittmar and Vogel (1968), Frank et al. (1982), Lepzelter et al. (1983), Morrison and Brand (1986), Grossman (1994), and Brand and Logan (personal communication, 2001).

seawater $^{87}Sr/^{86}Sr$ is recorded in the drop in ratios between the Darriwilian and early "Caradocian" from 0.7087 to 0.7078. Lowest ratios imply that seawater $^{87}Sr/^{86}Sr$ remained around 0.7078 to 0.7079 from the "Mohawkian" of North America to the Ordovician-Silurian boundary (see also Gao et al., 1996; Holmden et al., 1996; Qing et al., 1998), before rising again during the Early Silurian (Ruppel et al., 1996; Qing et al., 1998; Azmy et al., 1999).

The seawater Sr isotope record of the latest Cambrian through to the earliest Silurian is thus characterized by two periods of stasis during approximately 480 Ma −465 Ma and

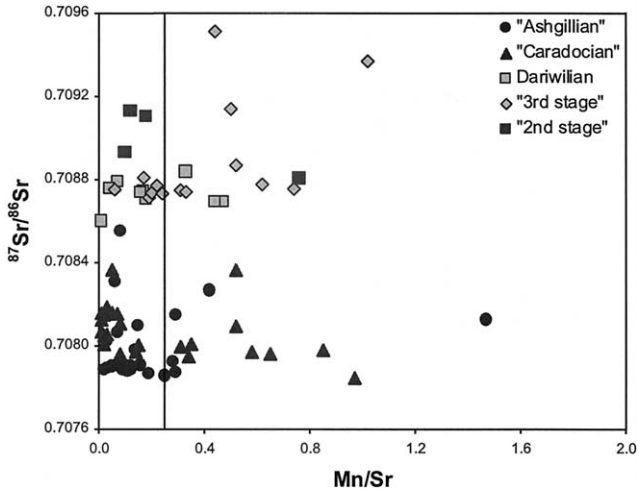

Fig. 5. Scatter diagram of Mn/Sr ratios (an indicator of diagenetic alteration) vs. $^{87}Sr/^{86}Sr$ in Ordovician brachiopod shells. The Mn/Sr = 0.25 dividing line represents a suggested maximum ratio for unaltered brachiopods (Fig. 3). Two extreme outliers from the Tremadocian have been omitted.

455 Ma −445 Ma, and two periods of decrease during approximately 500 Ma −480 Ma and 465 Ma −455 Ma (Fig. 8). The initial decrease occurred gradually after seawater $^{87}Sr/^{86}Sr$ had reached an all-time high during the Late Cambrian of 0.7092 or higher (Montañez et al., 1996; Ebneth et al., 2001). By contrast, the second decrease from 0.7087 to 0.7078 appears to have been much more rapid and has so far proven difficult to resolve adequately (Denison et al., 1998; Qing et al., 1998).

The three major sources for ocean strontium are river input of continental weathering products, marine carbonate diagenesis and dissolution, and hydrothermal exchange at plate boundaries (Veizer, 1989). Continental weathering of ancient crust supplies the more radiogenic end-member component, whereas submarine hydrothermal exchange and weathering of juvenile volcanic rocks supplies the less radiogenic end-member, averaging 0.704 (Faure, 1986). In general, the diagenesis and dissolution of geologically young carbonates, although representing a significant portion of the overall flux of Sr to the ocean, only serves to buffer seawater $^{87}Sr/^{86}Sr$ about the seawater value (Veizer, 1989). Therefore, the overall decrease in $^{87}Sr/^{86}Sr$ during the Ordovician Period is likely to reflect the progressively decreasing influence of continental crust-derived strontium, and conversely the progressively increasing influence of juvenile volcanic input and/or hydrothermal exchange on seawater $^{87}Sr/^{86}Sr$. Further analysis of this trend requires a closer look at the Ordovician geological record.

The geological record contains evidence for the orogenic uplift of great "Pan-African" mountain chains during the Terminal Proterozoic and Cambrian Periods, the weathering of which would have provided a source of the radiogenic Sr necessary to attain the Late Cambrian $^{87}Sr/^{86}Sr$ maximum (Montañez et al., 1996, 2000). It seems plausible, therefore, that the generally decreasing trend in $^{87}Sr/^{86}Sr$ during the Ordovician was at least partly a response to the lowering of tectonic uplift rates caused by the waning of Pan-African mountain-building (Qing et al., 1998). This explanation is consistent with the analysis of Richter et al. (1992) who report that the "areal extent of contractional deformation," which was calculated using present-day distributions of deformed rocks, decreased from a maximum value during the late Cambrian to reach an all-time minimum by the mid-Ordovician. However, gradually decreasing crustal weathering rates seem unlikely to explain the relatively sharp drop in seawater $^{87}Sr/^{86}Sr$ across the Middle–Late Ordovician transition, and it is perhaps more plausible that there was a second factor involved to cause this sudden change in the rate of decrease. One possible candidate may be found in the compilation of Ronov et al. (1980) who observed that the Ordovician was a time of high volcanism relative to the Cambrian and Silurian periods because the weathering of juvenile volcanic rocks contributes less radiogenic Sr to seawater. The Middle-early Late Ordovician, in particular, was a period of massive island-arc volcanism in Kazakhstan, deposits of which may reach up to 8 km in thickness (Nikitin et al., 1990). The main phase of the Taconian orogeny of eastern North America occurred around the same time and also resulted in massive island-arc volcanism related to the subduction of the Laurentian continental margin (Ettensohn, 1990; Wright et al., 2002). The relatively rapid weathering of these comparatively easily weathered volcanic rocks may have contributed to the Middle–Late Ordovician down-

Table 1. Isotopic data for Ordovician brachiopads from this study arranged according to Ordovician global stage time slices (Webby, 1998; Webby, personal communication). Two Silurian samples from Azmy et al. (1998) have also been included.

Stage	Time slice	Country	n_{Sr}	$^{87}Sr/^{86}Sr_{mean} \pm 1\sigma$[a]	Minimum	$n_{C,O}$	δ^{13}mean $\pm 1\sigma$	Max	Min	$\delta^{18}O_{mean} \pm 1\ \sigma$	Max	Min
Tremadocian	?	China	3	0.70902 ± 2	0.70901	3	−0.4 ± 0.4	0.0	−0.8	−9.1 ± 0.3	−8.9	−9.4
"Stage 2"	2a	China, Kazakhstan	4	0.70904 ± 10	0.70893	5	−1.1 ± 0.3	−0.7	−1.5	−10.1 ± 0.6	−9.5	−11.1
	2b	China, Kazakhstan	4	0.70904 ± 8	0.70888							
	2c	USA, Russia	6	0.70889 ± 13	0.70880	7	−1.0 ± 0.2	−0.6	−1.2	−8.8 ± 0.4	−8.2	−9.3
"Stage 3"	3a	USA, Australia, China	13	0.70890 ± 26	0.70873	26	−1.7 ± 0.6	−0.9	−3.0	−7.5 ± 0.5	−6.3	−9.0
	3b	Russia	5	0.70876 ± 4	0.70871	11	−0.4 ± 0.3	0.3	−0.7	−5.9 ± 0.2	−5.4	−6.3
Darriwilian	4a	China, USA	9	0.70875 ± 2	0.70873	20	−1.4 ± 0.7	−0.4	−2.5	−6.6 ± 0.7	−5.4	−8.0
	4b	USA, China	5	0.70875 ± 7	0.70870	6	−0.7 ± 1.6	+1.8	−1.9	−6.5 ± 1.0	−5.5	−7.8
	4c	USA	2	0.70863 ± 3	0.70860	2	−0.6 ± 0.2	−0.4	−0.6	−6.5 ± 0.2	−6.2	−6.5
	5a											
"Caradocian"	5b	USA	7	0.70819 ± 10	0.70815	14	−0.7 ± 0.5	+0.1	−1.2	−5.2 ± 0.7	−4.0	−6.2
	5b	USA	23	0.70803 ± 9	0.70785	31	0.0 ± 0.8	+1.2	−1.5	−5.6 ± 0.7	−4.2	−6.8
	5c	USA	2	0.70793 ± 3	0.70791	1	−2.1	—	—	−6.5	—	—
"Ashgillian"	5d	USA	7	0.70788 ± 6	0.70785	9	+0.1 ± 0.6	+1.3	−0.7	−4.8 ± 0.8	−3.5	−5.5
	6a											
	6b	China, USA	11	0.70792 ± 11	0.70784	16	+0.2 ± 0.3	+0.5	−0.4	−5.2 ± 1.2	−3.7	−6.9
	6c	Canada	20	0.70799 ± 21	0.70787	31	+1.6 ± 1.7	+5.8	+0.2	−3.2 ± 0.9	+0.2	−4.3
Llandoverian	1	Canada	3	0.70796 ± 4	0.70793	3	+1.1 ± 0.6	+1.50	+0.35	−3.2 ± 0.4	−2.70	−3.56

[a] 1σ value $\times 10^5$.
[b] extreme negative outliers have been omitted.

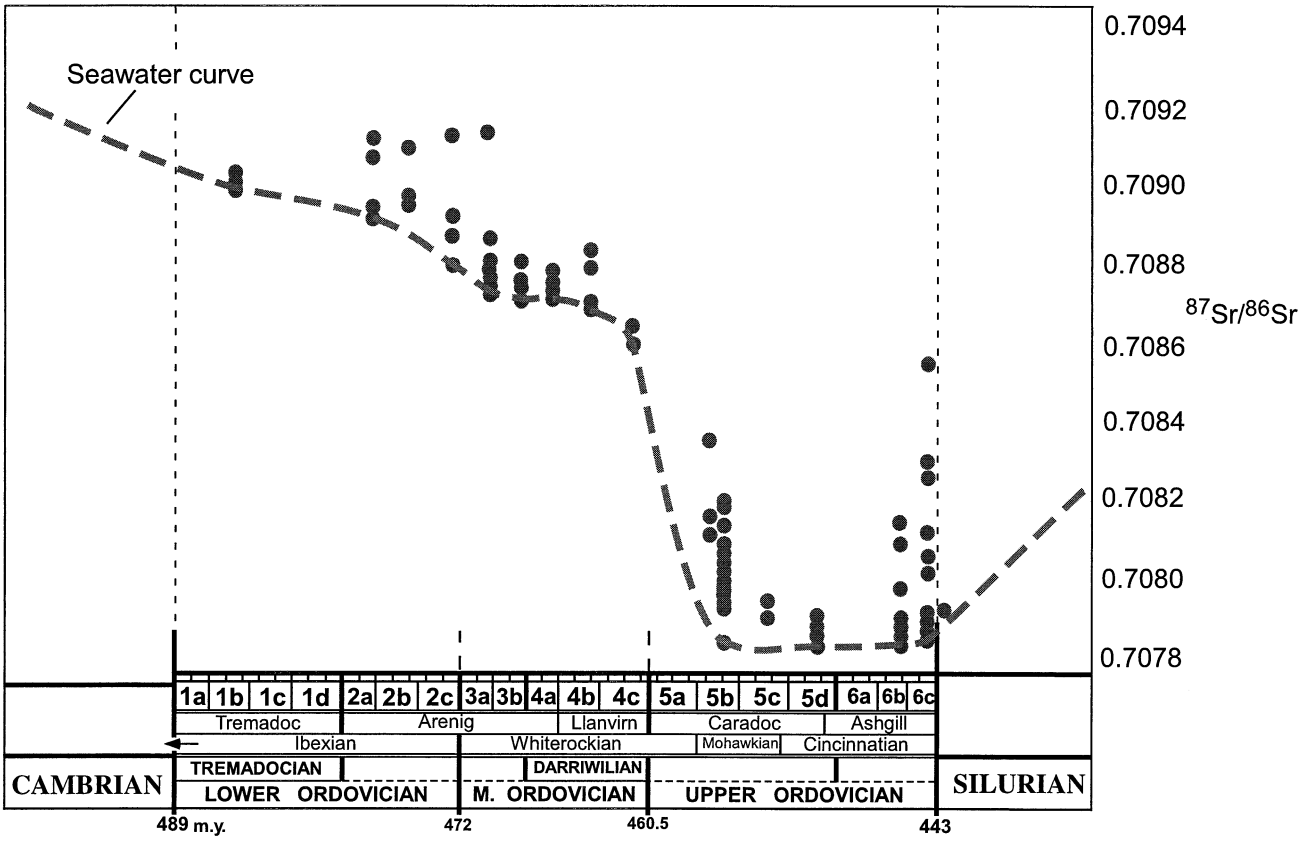

Fig. 6. Secular variation in $^{87}Sr/^{86}Sr$ of Ordovician brachiopods from this study arranged according to global time-slices, stages, and series (Webby, 1998; Webby, personal communication). For age assignments see text. Symbols are larger than the best scenario overall reproducibility of $\pm 25 \times 10^{-6}$ (Veizer et al., 1999; Ebneth et al., 2001); some points are hidden behind others. Dashed line joins lowest values for each sample suite and is our best approximation to seawater $^{87}Sr/^{86}Sr$. Seawater curve is taken from Veizer et al. (1999). Extreme outliers have been omitted. Age uncertainty of samples covers entire time-slice.

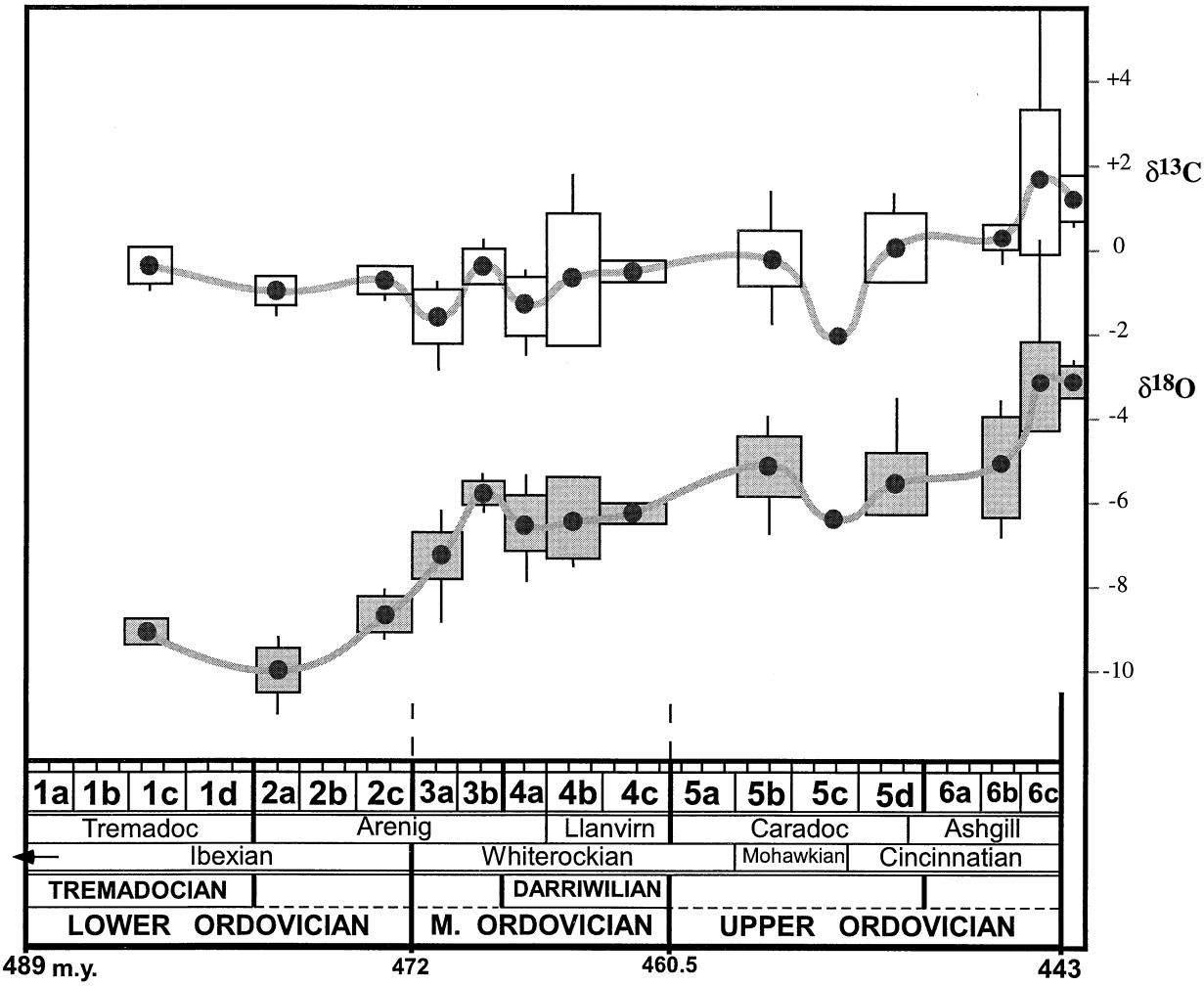

Fig. 7. Secular variation in $\delta^{13}C$ and $\delta^{18}O$ of Ordovician brachiopods from this study arranged according to global time-slices, stages, and series (Webby, 1998; Webby, personal communication). For age assignments see text. Boxes correspond to 1 standard deviation from the mean (black dot) for each time-slice, with horizontal bars showing minimum and maximum measured values.

turn. Thirdly, the Middle–Late Ordovician transition also coincides with a major transgression, possibly the largest in the Phanerozoic (Ross and Ross, 1992). Such a major eustatic sea-level event, in an ice cap–free world (Frakes et al., 1992), must have been related to tectonic events, most likely an acceleration in ocean spreading rates and/or an increase in the overall length of spreading ridges (Chen, 1990), which would also provide an appropriate mechanism to explain the decrease in seawater $^{87}Sr/^{86}Sr$ at this juncture. Such a global transgression would also have led to the drowning of huge cratonic areas, in effect shutting off the source of much radiogenic Sr (Denison et al., 1998; Qing et al., 1998).

Further constraints on the timing and rate of the Middle–Late Ordovician decrease in seawater $^{87}Sr/^{86}Sr$ are provided by the emerging global biostratigraphic framework (Webby, 1998), which can be calibrated in time by using the latest developments in Ordovician geochronology (Fig. 8; Webby, personal communication). From our study it can be seen that $^{87}Sr/^{86}Sr$ began to decrease from ~0.7087 during the deposition of the McLish Formation, Oklahoma, USA (*Glyptograptus teretiusculus Zone*) and reached a plateau ~0.70785 possibly during the deposition of the overlying Bromide Formation and at least before the deposition of the Bobycageon Formation in Kentucky, USA. This decrease is on the order of 850×10^{-6}, and covers 2 to 3 Ordovician time slices (Fig. 6), which, using current estimates, is likely to represent an interval of ~6 to 8 million years. The extraordinary rapidity of this major decrease, especially considering the long residence time of Sr in seawater of around 5 million years (Faure, 1986), defines the Middle–Late Ordovician transition as a major event in the Sr isotopic evolution of seawater. If our age estimates are correct, this event would be the most rapid change of this magnitude during the entire Phanerozoic, the major $^{87}Sr/^{86}Sr$ decreases of the Devonian and Permian having been considerably more prolonged (Veizer et al., 1997). These observations are consistent with a causal connection between the decrease in $^{87}Sr/^{86}Sr$ and the equally rapid contemporaneous transgression, which has been reported by Ross and Ross (1992) as possibly having

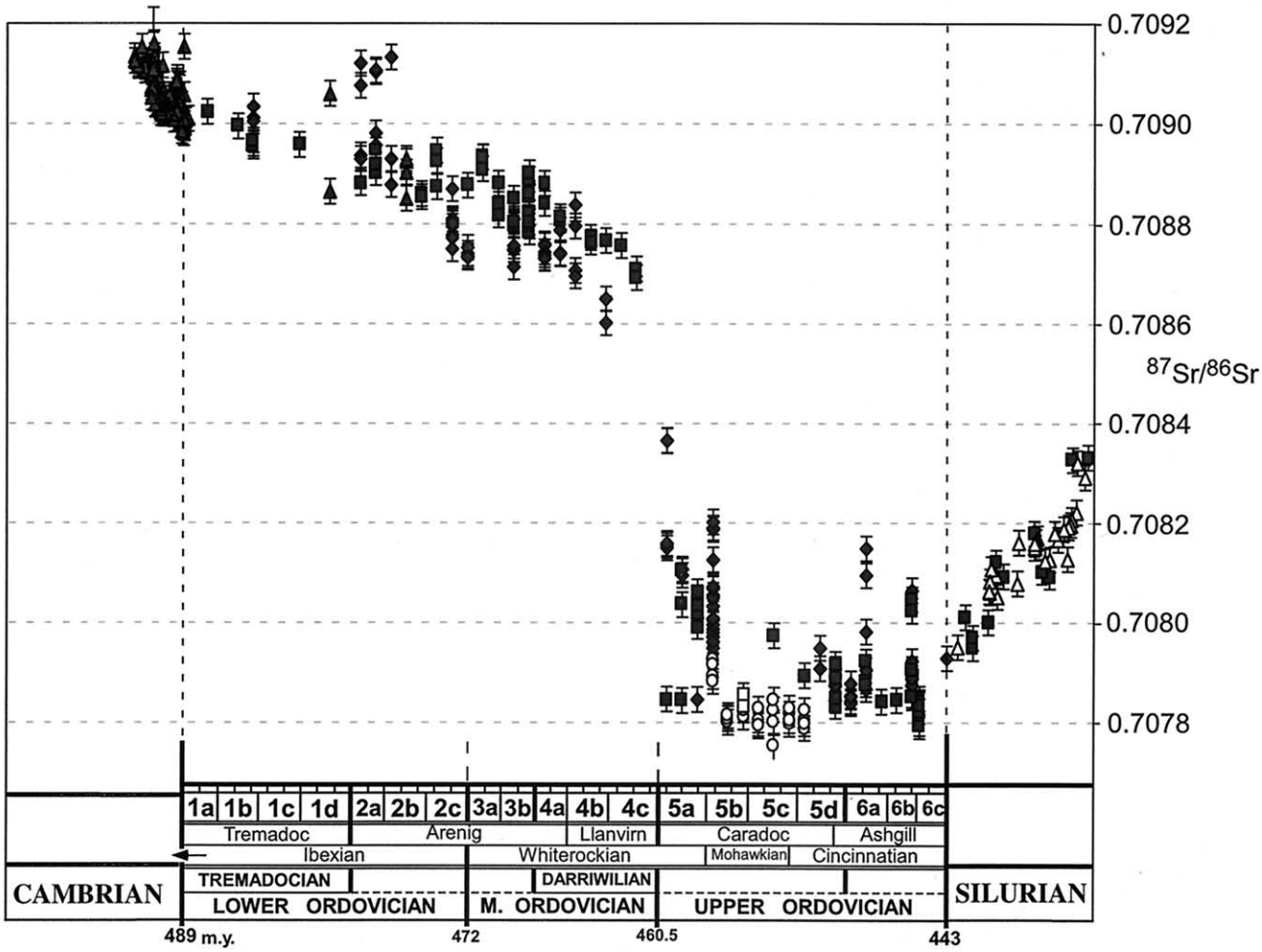

Fig. 8. Strontium isotopic variation in seawater during the Ordovician incorporating all currently available, apparently well-preserved brachiopod and carbonate component data: open triangles = Azmy et al. (1999), open circles = Gao et al. (1996), open squares = Wadleigh and Veizer (1992), filled triangles = Ebneth et al. (2001), filled squares = Qing et al. (1998), filled diamonds = this work. Vertical error bars correspond to a best scenario overall reproducibility of $\pm 25 \times 10^{-6}$ (Veizer et al., 1999; Ebneth et al., 2001).

been the largest of the entire Phanerozoic. In sum, the rapid decrease in seawater $^{87}Sr/^{86}Sr$ between ~465 and ~455 Ma is likely to have been the result of a combination of factors, including low collision, uplift and erosion rates, high levels of submarine hydrothermal cycling, and high rates of volcanic rock weathering. Such a combination of factors has previously been put forward as a plausible explanation for all the major $^{87}Sr/^{86}Sr$ lows during the Phanerozoic (Faure, 1986, p. 191).

6.2. Carbon Isotopes

Our C isotope data are inadequate to appropriately address the question of the relatively short-term $\delta^{13}C$ excursions that have been recognized in the Ordovician, but long-term trends can be discerned. Table 2 summarizes published oxygen isotope data for Ordovician marine carbonate components that we can place confidently into the emerging global biostratigraphic framework that is used throughout this paper. Previous stable isotope studies on bulk carbonate have documented a negative shift in $\delta^{13}C$ across the Cambrian–Ordovician boundary (Gao and Land, 1991; Ripperdan et al., 1992, 1993). Our Lower and Middle Ordovician brachiopod samples and those of Qing and Veizer (1994) nearly all yield negative $\delta^{13}C$ values, which is consistent with those previous findings. Thereafter, there appears to have been a general 2‰ shift to positive $\delta^{13}C$ by the Late Ordovician (Veizer et al., 1986; Marshall and Middleton, 1990; Middleton et al., 1991; Wadleigh and Veizer, 1992; Carden, 1995; Qing and Veizer, 1994; Gao et al., 1996; Ludvigson et al., 1996; Tobin and Walker, 1996; this paper; Table 2) with the likelihood of at least one significant $\delta^{13}C$ excursion up to +3‰ during the earliest Late Ordovician or early-mid "Caradoc" (Hatch et al., 1987; Patzkowsky et al., 1997; Ainsaar et al., 1999; Pancost et al., 1999). Our study and many others recognize a period of anomalously high $\delta^{13}C$ close to the Ordovician-Silurian boundary. This latest Ordovician $\delta^{13}C$ excursion has been documented globally using bulk carbonate, brachiopod, and marine cement samples (Marshall and Middleton, 1990; Long, 1993; Brenchley et al., 1991, 1994, 1997;

Table 2. Compilation of published isotope data for Ordovician brachiopods and other low-Mg calcite components.[a]

Stratigraphic interval	$n_{C,O}$	$\delta^{13}C$	Max	Min[b]	$\delta^{18}O$	Max	Min[b]	References
Late Cambrian	44	+0.5	+1.3	−0.7	−6.5	−5.6	−9.6	Wadleigh and Veizer (1992); Johnson and Goldstein (1993)
Tremadocian	7	−1.1	0.0	−2.5	−9.8	−8.9	−10.6	Qing and Veizer (1994); this paper
"Stage 2"	12	−1.0	−0.6	−1.5	−9.3	−8.2	−11.1	this paper
"Stage 3"	37	−1.3	+0.3	−3.0	−7.0	−5.4	−9.0	this paper
Darriwilian	88	−0.8	+1.8	−2.5	−7.2	−4.9	−8.6	Wadleigh and Veizer (1992); Qing and Veizer (1994); this paper
"Caradocian"	193	+0.1	+1.6	−2.1	−4.8	−3.1	−6.8	Wadleigh and Veizer (1992); Qing and Veizer (1994); Gao et al. (1996); this paper
"Ashgillian"	421	+2.0	+6.8	−2.5	−3.6	+0.6	−6.9	Veizer et al. (1986); Middleton et al. (1991); Wadleigh and Veizer (1992); Carden (1995); Qing and Veizer (1994); this paper
Llandoverian	49	+1.2	+2.9	0.0	−4.9	−2.7	−6.1	Azmy et al. (1998)

[a] Only data that we can confidently place into global stages have been included. "Stage 2" and "stage 3" data are also consistent with similarly aged data reported in Wadleigh and Veizer (1992) and Qing and Veizer (1994).

Marshall et al., 1997; Kump et al., 1999). Organic carbon studies have also confirmed a major change in seawater $\delta^{13}C$ at this juncture with positive excursions of 3‰ (Underwood et al., 1997) and 4‰ (Marshall et al., 1997; Wang et al., 1997) from several localities worldwide. The interpretation of this short-term excursion, which coincides with a global faunal extinction, major eustatic sea-level change, and glaciation, is beyond the scope of the present paper, which concentrates on longer-term isotopic shifts; see Brenchley et al. (1994) and Kump et al. (1999) for a full account of that debate.

6.3. Oxygen Isotopes

6.3.1. The Ordovician oxygen isotope record

The most striking feature of our oxygen isotope results is the increase in mean $\delta^{18}O$ from –10.1‰ in time-slice 2a (Table 1) to −3.2‰ in the *N. extraordinarius* Zone of the uppermost Ordovician. Table 2 summarizes published oxygen isotope data for Ordovician marine calcite components that we can place confidently into the emerging global biostratigraphic framework that is used throughout this paper. Together, these data reveal a rise in mean $\delta^{18}O$ from –9.8‰ in the Tremadocian to –3.6‰ in the upper "Ashgillian," identical to the trend in our data (Fig. 7). Diagenetic alteration, which has been suggested to be the prime cause of this rise (Land, 1995), most commonly depletes calcite in ^{18}O (Hudson, 1977). Therefore, maximum $\delta^{18}O$ values are frequently taken as the best approximation to primary values of calcites in equilibrium with seawater $\delta^{18}O$ (Gao et al., 1996). Table 2 shows that $\delta^{18}O$ maxima also increase greatly through the Ordovician from −8.9‰ to +0.6‰.

We acknowledge that the current database is heavily biased toward the Upper Ordovician. The Lower Ordovician, in particular, suffers from a lack of isotope data and poor biostratigraphic resolution that needs to be remedied in future studies. However, although data are relatively scarce, 226 marine calcite component samples (and numerous bulk carbonates) have been analyzed for stable isotopes from the Upper Cambrian to the Middle Ordovician. To our knowledge, none of those $\delta^{18}O$ values exceed –5.4‰ for this entire interval; some higher values have been reported from uppermost middle Ordovician calcite cements (Grover, 1981, and brachiopods (Wadleigh and Veizer, 1992), but those data would now be considered to belong to the Upper Ordovician. By contrast, Upper Ordovician samples are rarely more depleted than −5‰ (Tables 1 and 2), implying a clear switch in calcite $\delta^{18}O$ between 465 and 455 Ma, as well as an earlier, extended period of ^{18}O depletion lasting over 50 million years. Possible controls on this long-term trend are discussed below.

6.3.2. Diagenetic alteration

The issue of diagenetic resetting of $\delta^{18}O$ in low-Mg calcitic phases was discussed in detail in our earlier publications (Azmy et al., 1998; Bruckschen et al., 1999; Veizer et al., 1999). Only a few lowermost Ordovician brachiopod samples could be analyzed during the course of this study. These Mg, Mn, and Fe-rich and Sr-poor samples from the Tremadocian stage have clearly not retained their primary trace element compositions (Appendix A1; Fig. 4) and so the primary nature of their stable isotope compositions is correspondingly open to question. Qing and Veizer (1994) reached the same conclusion with regard to their ^{18}O-depleted Lower Ordovician samples (p. 4433) and this conclusion is strengthened by slightly older, but considerably less depleted, calcite $\delta^{18}O$ values from the literature (Johnson and Goldstein, 1993). Those $\delta^{18}O$ data from 21 low-Mg calcite cement samples from the uppermost Cambrian (Wilberns Formation, Texas, USA) depict a narrow range between −6.2‰ and –5.6‰ (Table 2), and are at the high range of reported bulk $\delta^{18}O_{calcite}$ data for the Cambrian–Ordovician boundary, that is, between −11‰ and −6‰ (Gao and Land, 1991; Ripperdan et al., 1992, 1993; Ripperdan and Miller, 1995). In the absence of any further $\delta^{18}O$ data for lowermost Ordovician brachiopods and well-preserved calcite components, we prefer to err on the side of caution and tentatively assume that our Tremadocian samples yield altered $\delta^{18}O$ values.

By contrast, it is more difficult to recognize the effects of diagenetic alteration in our post-Tremadocian samples. In fact, several arguments permit the conclusion that, overall, ^{18}O-depleted values for the Lower and Middle Ordovician are primary: 1) No $\delta^{18}O_{calcite}$ values higher than –5‰ have been

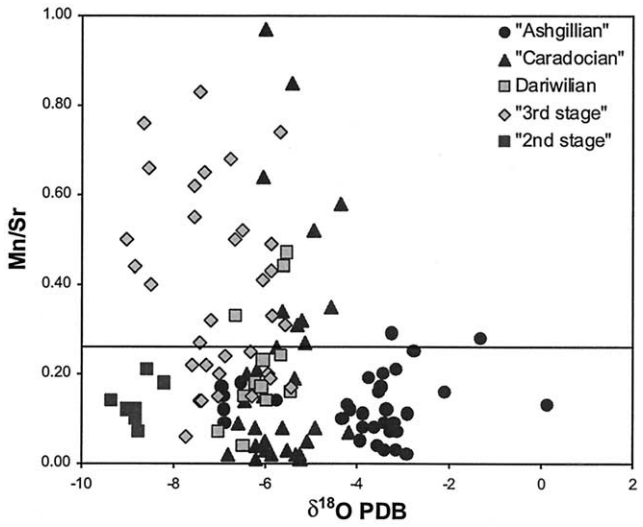

Fig. 9. Scatter diagram of Mn/Sr ratios (an indicator of diagenetic alteration) vs. $\delta^{18}O$ in Ordovician brachiopod shells. The Mn/Sr = 0.25 dividing line represents a suggested maximum ratio for unaltered brachiopods (Fig. 4). Two extreme outliers from the Tremadocian have been omitted. Note that both "2nd stage" and "Ashgillian" samples appear from trace element concentrations to be well preserved despite their contrasting $\delta^{18}O$ values.

reported from the entire Upper Cambrian to uppermost middle Ordovician interval. Although diagenetic alteration is likely to affect entire suites of samples, it cannot easily explain wholesale ^{18}O depletion for all carbonates deposited during a ~50 Ma time-span. More data are still required though to completely exclude the existence of more enriched $\delta^{18}O$ values over that interval. 2) Cathodoluminescence and SEM studies on the microstructure of our samples reveal no significant differences between Upper Ordovician and Lower Ordovician brachiopods despite considerable differences in $\delta^{18}O$ (Fig. 3; cf. Carden, 1995). Sample Alb06b (Fig. 3) is a case in point. Considering that oxygen represents 60% of all the atoms in calcite, resetting of such a magnitude could be achieved only by wholesale dissolution and reprecipitation of the shells, a feat that would surely have resulted in textural destruction and resetting of chemical and isotopic attributes. 3) Figure 9 shows $\delta^{18}O$ data for our brachiopods plotted against Mn/Sr, which can sometimes be a useful indicator of diagenetic alteration in brachiopod shells (Veizer et al., 1999). There appears to be no correlation between low $\delta^{18}O$ and high Mn/Sr ratios within stages or in the data as a whole that could be attributed to secondary alteration. We note, however, that this might also indicate that diagenetic alteration occurred under relatively oxidizing conditions, which made manganese insoluble. 4) Pristine seawater $^{87}Sr/^{86}Sr$ ratios, which are not always recorded in even texturally well-preserved brachiopods due to microimpurities or diagenetic alteration, have been retained by several ^{18}O-depleted Lower and Middle Ordovician sample suites (Fig. 3; Appendix). 5) It is usual for fossil brachiopods from the uppermost Ordovician and at other times, too, to preserve the oxygen isotopic signature of glaciation (Brenchley et al., 1994; Azmy et al., 1998; Mii et al., 2001; this paper), something that would not be expected were brachiopods susceptible to such pervasive and systematic isotopic alteration. 6) The trend toward ^{18}O enrichment during the Ordovician is found in both mean and maximum (and presumably least altered) $\delta^{18}O$ values. Therefore, unless new, less ^{18}O-depleted data from the Lower Ordovician are reported in the future, it is hard to avoid the conclusion that ^{18}O depletion is a primary feature of Early and Middle Ordovician brachiopods. 7) Lastly, it has recently been recognized that Lower-Upper Ordovician ^{18}O enrichment corresponds to one of four climatically related $\delta^{18}O$ cycles during the Phanerozoic (Veizer et al., 2000). To our minds, it is not feasible that such global cycles would be recognizable were diagenetic alteration the major controlling factor on fossil brachiopod $\delta^{18}O$. For this to be the case, Upper Ordovician brachiopods worldwide, for example, would have to be systematically better preserved than their underlying Lower and Middle Ordovician, as well as their overlying Silurian counterparts (Azmy et al., 1998), which seems implausible.

We acknowledge that none of these arguments unequivocally excludes the possibility of significant alteration of $\delta^{18}O$ values in our post-Tremadocian brachiopod samples and those reported in the literature, but their combined weight makes that alternative less likely. Therefore, we consider the ^{18}O depletion in Lower and Middle Ordovician brachiopods ($<-5.4‰$) relative to Upper Ordovician brachiopods ($<-3‰$) and the depletion of these latter brachiopods relative to those from the uppermost Ordovician ($<+1‰$) to be primary.

6.3.3. Paleogeographic and seasonal variation

The paleogeographic reconstruction of the continents during the Early Ordovician (Fig. 2) illustrates that most of the investigated brachiopods would have been living at equatorial latitudes. The one possible exception to this would be the Russian brachiopods from the Volkhov and Leetse Formations. Paleogeographic variation in present-day surface seawater $\delta^{18}O$ amounts to 3‰ for regions within latitudes 50°N to 50°S (Schmidt, 1999; Bigg and Rohling, 2000). Previous studies on tropical Carboniferous brachiopods have found paleogeographic variation in the mean $\delta^{18}O$ of almost 2‰ (Grossman et al., 1996; Mii et al., 2001), and $\delta^{18}O$ variation in present-day tropical brachiopods can be as much as 3 to 5‰ (Bruckschen, personal communication, 2001; Brand and Morgan, personal communication, 2001). In addition to these factors, seasonal variations of <1‰ can be expected (Mii and Grossman, 1994). Such paleogeographic and seasonal variations do not depend solely on the distance from the equator but on paleocurrents, temperature, and salinity, making generalizations about $\delta^{18}O$ variation in the ancient ocean difficult. A combination of these influences can accommodate the differences in mean $\delta^{18}O$ that we observe within each time-slice of the Ordovician as well as differences between sampling sites of approximately the same age, which are consistently less than 3‰ (Appendix A1). However, such paleogeographic variations fail to explain the absolute ^{18}O depletion during the Early and Middle Ordovician relative to the Late Ordovician, which is observed in paleogeographically widespread samples.

6.3.4. Glaciation

Both $\delta^{13}C$ and $\delta^{18}O$ peak within the lower part of the Hirnantian substage of the uppermost "Ashgillian," reaching

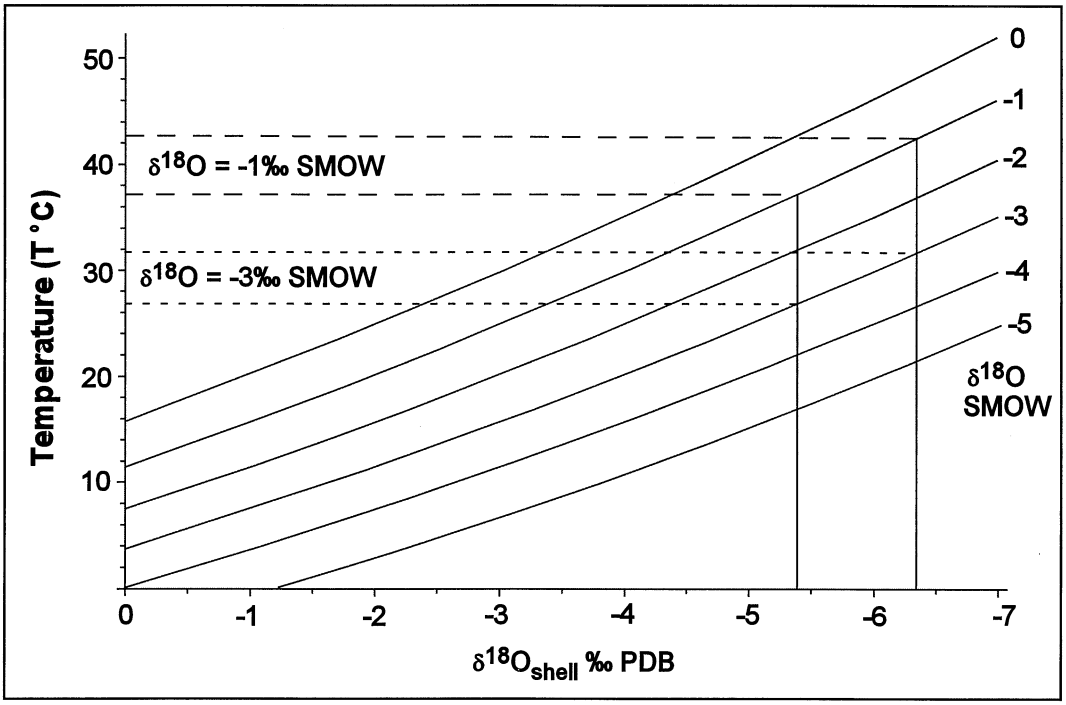

Fig. 10. Temperature vs. calcium carbonate shell $\delta^{18}O$ (PDB) for various values of seawater $\delta^{18}O$ (SMOW) assuming an ice-cap free world. Even maximum $\delta^{18}O$ values for the Early Ordovician and early Middle Ordovician (−5.4‰ and −6.3‰, respectively) yield unrealistic minimum seawater temperatures (37°C –43°C) if $\delta^{18}O_{seawater}$ was ≥−1‰ SMOW, while $\delta^{18}O_{seawater}$ of <−3‰ SMOW yields more plausible minimum tropical sea-surface temperatures of 27°C –32°C.

+7‰ and 0‰ Pee Dee Belemnite (PDB), respectively (Marshall and Middleton, 1990; Middleton et al., 1991; Wang et al., 1993; Carden, 1995; Brenchley et al., 1997; Kump et al., 1999; this paper). Marshall et al. (1997) observe further that the range of well-preserved brachiopod $\delta^{18}O$ values is identical worldwide on either side of the lower Hirnantian (−5‰ to –3‰), and this is confirmed by our compilation of literature data (Table 2). This is consistent with the faithful preservation of the glacial isotopic signature of early Hirnantian glaciation (Brenchley et al., 1997; Marshall et al., 1997). Preferential storage of ^{16}O due to glaciation can increase seawater $\delta^{18}O$ by up to 2 to 3‰ assuming an originally ice-free world (Muehlenbachs, 1998) and so could feasibly be the sole cause of this short-lived excursion. However, considering that all of this predicted effect on $\delta^{18}O$ is restricted to the latest Ordovician, glaciation is not likely to be an adequate explanation for the ^{18}O depletion of Lower and Middle Ordovician brachiopods relative to Upper Ordovician and Lower Silurian brachiopods.

6.3.5. Paleotemperature

Assuming that Ordovician surface water $\delta^{18}O$ (seawater, groundwater, and ice) and equatorial temperatures were identical to those of today, i.e., −1‰ standard mean ocean water (SMOW) (Muehlenbachs, 1998) and 23°C to 27°C (Azmy et al., 1998), respectively, it would appear that Lower–Middle Ordovician brachiopods and marine calcite components are anomalously depleted in ^{18}O (Veizer et al., 1986). This enigma could be resolved if Ordovician equatorial seawater temperatures were higher or seawater $\delta^{18}O$ was lower than today. Because no marine calcite $\delta^{18}O$ value has been reported for the entire Cambrian–Middle Ordovician that is higher than –5.4‰ (Table 2), this puts a firm lower limit on sea-surface temperatures of ~37°C assuming a seawater isotopic composition of −1‰ (Fig. 10). However, most Lower Ordovician $\delta^{18}O$ values are significantly lower than this upper limit. For example, maximum $\delta^{18}O$ for time-slice 3a is −6.3‰, which would correspond to *minimum* sea-surface temperatures of 43°C. Such high minimum water temperatures are unrealistic because protein molecules cannot withstand continuous temperature stress in excess of 37°C (Milliman, 1974; Brock, 1985). To attain more realistic minimum temperatures, such as 27°C to 32°C, it is necessary to accept that seawater $\delta^{18}O$ evolved during geological history (Tobin et al., 1996; Wallmann, 2001), being no higher than about −3‰ SMOW during the Late Cambrian to Middle Ordovician interval (Fig. 10).

Both mean and maximum calcite $\delta^{18}O$ values increase by around 2 to 3‰ between the Lower and the Upper Ordovician (Table 2). From the available data, it would appear that much of this change in maximum $\delta^{18}O$ occurred around the Middle–Late Ordovician transition over a period of less than 10 million years. Figure 10 illustrates how the rise in calcite $\delta^{18}O$ through the Ordovician could possibly be explained by a drop in minimum tropical sea-surface temperatures from 27°C to 32°C to 16° to 25°C if seawater $\delta^{18}O$ were −3‰. This interpretation is further supported by the detailed isotopic work of Tobin et al. (1996), and the sedimentological work of Frakes et al. (1992)

who identified a cool climatic mode lasting around 35 Ma starting in the "Caradocian," intensifying in the "Ashgillian," and waning through the Silurian. However, such a large decrease in tropical sea surface temperatures seems to be unrealistic as this would surely have led to widespread glaciation during the "Caradocian," but we know that glaciation did not occur until the late "Ashgillian" (Brenchley et al., 1991, 1994). One reasonable alternative would be that decreasing tropical temperatures were accompanied by rising seawater $\delta^{18}O$ at this time. Veizer et al. (2000) report several such temperature-related excursions in calcite $\delta^{18}O$ of ~2 to 3‰ that correspond to the icehouse parts of icehouse/greenhouse cycles superimposed on an overall rising seawater $\delta^{18}O$ trend. The possibility that seawater $\delta^{18}O$ changed significantly during the Ordovician is explored further below.

6.3.6. Changing seawater $\delta^{18}O$

The isotopic composition of seawater is mainly controlled by isotopic exchange reactions with oceanic crust (Muehlenbachs and Clayton, 1976; Walker and Lohmann, 1989; Muehlenbachs, 1998; Wallmann, 2001). In upper crustal levels, low-temperature alteration by seawater circulation decreases the $\delta^{18}O$ level of seawater by increasing the $\delta^{18}O$ value of the rock. Deeper in the crustal section, at temperatures of 350°C, the polarity of exchange reverses and the $\delta^{18}O$ of seawater is increased at the expense of the rock (Bowers and Taylor, 1985). Therefore, increasing seawater $\delta^{18}O$ during the Ordovician might result from a decrease in low-temperature alteration ($<\sim$250°C). Model studies show that the depths of the "isotopic neutral point," separating the ^{18}O-enriched upper crust and the ^{18}O-depleted deeper crustal levels, might be controlled by the intensity and duration of ridge-flank circulation because low-temperature alteration in aging crust overprints the isotopic signature of ocean crust sections previously altered by high-temperature fluids (Lécuyer and Allemand, 1999), whereas the nature of ridge-flank circulation is controlled in part by the presence or absence of a sedimentary cover. In the present ocean, the flanks of midocean ridges are generally covered with carbonate and siliceous oozes composed of the remains of planktonic organisms, which have the effect of inhibiting vertical fluid flow and limit this flow to outcropping basement highs or volcanic structures, which then act as conduits for fluid recharge and discharge (Fisher and Becker, 2000). This mode of convection effectively cools large portions of ocean crust because conduction allows for a rapid heat transfer between high permeability zones and the surrounding crust (Stein et al., 1995).

Significantly, pelagic skeletal materials first appeared only towards the end of the Precambrian, whereas the greatest expansion of pelagic, skeletal forms took place during the very latest Cambrian and during the Ordovician period. It would seem likely that before this evolutionary expansion hydrothermal alteration would not have been restricted to occasional conduits, leading to more regional heat discharge and alteration. Therefore, the effect of thickening the sediment cover on ridge flanks during the Late Cambrian–Ordovician expansion of pelagic skeletal organisms would have been to increase surface alteration of ocean crust, which could be considered a possible mechanism for increasing seawater $\delta^{18}O$ during the early Paleozoic. The precise working and viability of this mechanism does not fall within the scope of the present paper but is explored further in a recently submitted paper by Klaus Wallmann, Shields, and Veizer. But we might ask the question: could changing seawater $\delta^{18}O$ potentially explain the entire 2–3‰ increase around the Middle–Late Ordovician transition?

Previous models have emphasized the sluggishness of seawater $\delta^{18}O$ to change; for example, Gregory (1991) calculated that $\delta^{18}O$ could not change by more than 2‰ over 100 Ma. However, Lécuyer and Allemand (1999) claim that there are still too few data to assess this conclusion; their model allows for the occurrence of similar changes in seawater $\delta^{18}O$ within a much shorter time frame (5 to 50 Ma) and make the point that seawater $\delta^{18}O$ would change more rapidly during periods of high ocean spreading rates. As argued above, the Middle–Late Ordovician interval is likely to have covered a period of intense ocean spreading, which would permit a more rapid reaction of seawater $\delta^{18}O$ to changes in the $^{18}O/^{16}O$ budget. However, because of the lack of data on this subject we leave the question of the possible rates of change of seawater $\delta^{18}O$ during the Ordovician open to discussion, while noting the likelihood that seawater $\delta^{18}O$ did indeed rise at least gradually during the early Palaeozoic (Veizer et al., 2000; Wallmann, 2001).

7. CONCLUSIONS

Most Ordovician brachiopod shells from our study yield stratigraphically consistent $\delta^{13}C$, $\delta^{18}O$ and $^{87}Sr/^{86}Sr$ isotopic trends, which we interpret in most cases to reflect the primary isotopic compositions of the precipitated calcite. A major shift in brachiopod shell isotopic composition can be identified during the Middle–Late Ordovician: an increase in mean $\delta^{13}C$ of over 1‰, an increase in both mean and maximum $\delta^{18}O$ of 2 to 3‰, and a decrease in $^{87}Sr/^{86}Sr$ from 0.70875 to 0.70785.

It is difficult to explain Early Ordovician ^{18}O depletion without allowing seawater $\delta^{18}O$ to have been at least 3‰ more depleted than present-day seawater. Decreasing temperatures around the Middle–Late Ordovician boundary are not enough to explain the major increase in calcite $\delta^{18}O$ at that juncture. However, decreasing temperatures together with a steady increase in seawater $\delta^{18}O$ could be an adequate explanation.

The apparent coupling of the Sr and O isotopic systems around the Middle–Late Ordovician transition suggests that both systems had similar controls at that time, while the contemporaneous, major sea-level rise suggests that any overriding control was related to ocean spreading rates.

Acknowledgments—This study was made possible by the generously provided expertise of several colleagues to whom we are extremely grateful: P. Brenchley (Univ. Liverpool); R. Cocks (Natural History Museum, London); J. Chaplin and B. Fay (Oklahoma Geol. Surv.); Jisuu-jin (Univ. Western Ontario); P. Copper (Laurentian Univ.); S. Ebneth (Ruhr Univ., Bochum); L. Holmer (Uppsala Univ.); N. Hughes (Cincinnati Mus.); L. Hintze and K. Rigby (Brigham Young Univ.); J. Laurie (AGSO, Canberra); M. Megl (W. Bohemian Univ., Czech Republic); L. Popov (VSEGEI, Russia); W. Sweet (Univ. Columbia, Ohio); T. Thompson (Dept. Nat. Res., Missouri); and Yuan Wen-wei and Chen Xu (Nanjing). We are also extremely grateful to the following people who gave of their time to help improve this manuscript: S. Finney (Cal. State Univ., Long Beach), J. Marshall (Univ. Liverpool), B. Webby (Macquarie Univ.), M. Joachimski (Univ. Erlangen), and L. Kump (Penn. State Univ.). This project was supported financially by the Deutsche Forschungsgemeinschaft (Leibnitz Prize and grant Ve

112/7-2) and by the Natural Sciences and Engineering Council of Canada to J. Veizer. The suggestion that increasing pelagic sedimentation might have caused a change in seawater $\delta^{18}O$ derives from discussions with K. Wallmann (GEOMAR).

Associate editor: L. R. Kump

REFERENCES

Ainsaar L., Meidla T., and Martma T. (1999) Evidence for a widespread carbon isotopic event associated with late Middle Ordovician sedimentological and faunal changes in Estonia. *Geol. Mag.* **136,** 49–62.

Azmy K., Veizer J., Bassett M. G., and Copper P. (1998) Oxygen and carbon isotopic compositions of Silurian brachiopods: Implications for coeval seawater and glaciations. *GSA Bulletin* **110,** 1499–1512.

Azmy K., Veizer J., Wenzel B., Bassett M. G., and Copper P. (1999) Silurian strontium isotope stratigraphy. *GSA Bulletin* **111,** 475–483.

Bigg G. R. and Rohling E. J. (2000) An oxygen isotope data set for marine waters. *J. Geophys. Res.* **105,** 8527–8535.

Birck J. L. (1986) Precision K-Rb-Sr isotopic analyses: Application to Rb-Sr chronology. *Chem. Geol.* **56,** 73–88.

Bowers TS. and Taylor HP. Jr. (1985) An integrated chemical and stable-isotope model of the origin of midocean ridge hot-spring systems. *J. Geophys. Res.* **90,** 12583–12606.

Brand U. and Veizer J. (1980) Chemical diagenesis of a multicomponent carbonate system: 1. Trace elements. *J. Sediment. Petrol.* **50,** 987–997.

Brenchley P. J., Marshall J. D., Carden G. A. F., Robertson D. B. R., Long D. G. F., Meidla T., Hints L., and Anderson T. F. (1994) Bathymetric and isotopic evidence for a short-lived Late Ordovician glaciation in a greenhouse period. *Geology* **22,** 295–298.

Brenchley P. J., Marshall J. D., Hints L., and Nõlvak J. (1997) New isotopic data solving an old biostratigraphic problem: The age of the upper Ordovician brachiopod *Holorhynchus giganteus*. *J. Geol. Soc. (London)* **154,** 335–342.

Brenchley P. J., Romano M., Young T. P., and Storch P. (1991) Hirnantian glaciomarine diamictites—evidence for the spread of glaciation and its effect on Upper Ordovician faunas. In *Advances in Ordovician Geology* (eds. C. R. Barnes and S. H. Williams), Geological Survey of Canada, Paper **90–9,** pp. 323–336.

Brock T. D. (1985) Life at high temperatures. *Science* **230,** 132–138.

Bruckschen P., Oesmann S., and Veizer J. (1999) Isotope stratigraphy of the European Carboniferous: Proxy signals for ocean chemistry, climate and tectonics. *Chem. Geol.* **161,** 127–163.

Burke W. H., Denison R. E., Hetherington E. A., Koepnik R. B., Nelson H. F., and Otto J. B. (1982) Variations of seawater $^{87}Sr/^{86}Sr$ through Phanerozoic time. *Geology* **10,** 516–519.

Carden G. A. F. (1995) Stable isotopic changes across the Ordovician-Silurian boundary. Unpublished Ph.D. thesis, University of Liverpool, UK.

Carpenter S. J. and Lohmann K. C. (1995) $\delta^{18}O$ and $\delta^{13}C$ values of modern brachiopod shells. *Geochim. Cosmochim. Acta* **59,** 3749–3764.

Chen J. (1990) Bathymetric biosignals and Ordovician chronology of eustatic variations. In *Advances in Ordovician Geology* (eds. C. R. Barnes and S. H. Williams), Geological Survey of Canada, Paper **90–9,** pp. 299–311.

Clayton R. M. and Degens E. T. (1959) Use of C isotope analyses for differentiating fresh-water from marine sediments. *AAPG Bulletin* **42,** 890–897.

Denison R. E., Koepnik R. B., Burke W. H., and Hetherington E. A. (1998) Construction of the Cambrian and Ordovician seawater $^{87}Sr/^{86}Sr$ curve. *Chem. Geol.* **152,** 325–340.

Diener A., Ebneth S., Veizer J., and Buhl D. (1996) Strontium isotope stratigraphy of the Middle Devonian: Brachiopods and conodonts. *Geochim. Cosmochim. Acta* **60,** 639–652.

Dittmar H. and Vogel K. (1968) Die Superenelemente Mangan und Vanadium in Brachiopoden-Schalen in Abhängigkeit vom Biotop. *Chem. Geol.* **3,** 95–110.

Ebneth S., Shields G. A., Veizer J., Miller J. F., and Shergold J. H. (2001) High-resolution strontium isotope stratigraphy across the Cambrian-Ordovician transition. *Geochim. Cosmochim. Acta* **65,** 2273–2292.

Ettensohn F. R. (1990) Flexural interpretation of relationships between Ordovician tectonism and stratigraphic sequences, central and southern Appalachians, USA. In *Advances in Ordovician Geology* (eds. C. R. Barnes and S. H. Williams), Geological Survey of Canada, Paper **90–9,** pp. 213–224.

Faure G. (1986) *Principles of Isotope Geology*. Wiley.

Fisher A. T. and Becker K. (2000) Channelized fluid flow in oceanic crust reconciles heat-flow and permeability data. *Nature* **403,** 71–74.

Fortey R. A., Harper D. A. T., Ingham J. K., Owen A. W., and Rushton A. W. A. (1995) A revision of Ordovician series and stages from the historical type area. *Geol. Mag.* **132,** 15–30.

Frakes L. A., Francis J. E., and Syktus J. I. (1992) *Climate Modes of the Phanerozoic*. Cambridge University Press.

Frank J. R., Carpenter A. B., and Oglesby T. W. (1982) Cathodoluminescence and composition of calcite cement in the Taum Sauk Limestone (Upper Cambrian), southeast Missouri. *J. Sed. Pet.* **52,** 631–638.

Gao G., Dworkin S. I., Land L. S., and Elmore R. D. (1996) Geochemistry of Late Ordovician Viola Limestone, Oklahoma: Implications for marine carbonate mineralogy and isotopic compositions. *J. Geol.* **104,** 359–367.

Gao G. and Land L. S. (1991) Geochemistry of Cambrian-Ordovician Arbuckle Limestone, Oklahoma: Implications for diagenetic ^{18}O alteration and secular ^{13}C and $^{87}Sr/^{86}Sr$ variation. *Geochim. Cosmochim. Acta* **55,** 2911–2920.

Gregory R. T. (1991) Oxygen isotope history of seawater revisited: timescales for boundary event changes in the oxygen isotope composition of seawater. In Stable isotope geochemistry: A Tribute to Samuel Epstein (eds. Taylor H.P., O'Neil J.R., and Kaplan I.R.). Geochemical Society Special Publication, pp. 65–76.

Grossman E. L. (1994) The carbon and oxygen isotope record during the evolution of Pangea: Carboniferous to Triassic. In *Pangea: Paleoclimate, Tectonics, and Sedimentation During Accretion, Zenith, and Breakup of a Supercontinent*. (ed. G. D. Klein). Geol. Soc. America Special Paper 288, pp. 207–228.

Grossman E. L., Mii H., Zhang C., and Yancey T. E. (1996) Chemical variations in Pennsylvanian brachiopod shells: Miagenetic, taxonomic, microstructural, and seasonal effects. *J. Sed. Res.* **66,** 1011–1022.

Grover G. A. Jr. (1981) Cement types and cementation patterns of Middle Ordovician ramp-to-basin carbonates. Ph.D. thesis, Virginia Polytechnic Institute and State University.

Hatch J. R., Jacobson S. R., Witzke B. J., Risatti J. B., Anders D. E., Watney W. L., Newell K. D., and Vuletich A. K. (1987) Possible Late Middle Ordovician organic carbon isotope excursion: Evidence from Ordovician oils and hydrocarbon source rocks, mid-continent and east-central USA. *AAPG Bulletin* **71,** 1342–1354.

Holmden C., Creaser R. A., Muehlenbachs K., Bergstrom S. M., and Leslie S. A. (1996) Isotopic and elemental systematics of Sr and Nd in Ordovician biogenic apatites: Implications for paleoseawater studies. *Earth Planet. Sci. Lett.* **142,** 425–437.

Hudson J. D. (1977) Stable isotopes and limestone lithification. *J. Geol. Soc. (London)* **133,** 637–660.

Johnson W. J. and Goldstein R. H. (1993) Cambrian seawater preserved as inclusions in marine low-Mg calcite cement. *Nature* **232,** 335–337.

Kump L., Arthur M. A., Patzkowsky M. E., Gibbs M. T., Pinkus D. S., and Sheehan P. M. (1999) A weathering hypothesis for glaciation at high atmospheric pCO_2 during the Late Ordovician. *Palaeogeog. Palaeoclimat. Palaeoecol.* **152,** 173–187.

Land L. S. (1995) Oxygen and carbon isotopic composition of Ordovician brachiopods: Implications for coeval seawater: Discussion. *Geochim. Cosmochim. Acta* **59,** 2843–2844.

Lécuyer C. and Allemand P. (1999) Modelling of oxygen isotope evolution of seawater: Implications for the climate interpretation of the $\delta^{18}O$ of marine sediments. *Geochim. Cosmochim. Acta* **63,** 351–361.

Lepzelter C. G., Anderson T. F., and Sandberg P. A. (1983) Stable isotope variation in modern articulate brachiopods (abs.). *AAPG Bulletin* **67,** 500–501.

Long D. G. F. (1993) Oxygen and carbon isotopes and event stratigraphy near the Ordovician-Silurian boundary, Anticosti Island, Quebec. *Palaeogeogr., Palaeoclimatol., Palaeoecol.* **104,** 49–59.

Lowenstam H. A. (1961) Mineralogy, $^{18}O/^{16}O$ ratios, and strontium and magnesium contents of recent and fossil brachiopods and their bearing on the history of oceans. *J. Geol.* **69,** 241–260.

Ludvigson G. A., Jacobson S. R., Witzke B. J., and Gonzalez L. A. (1990) Carbonate component chemostratigraphy and depositional history of the Ordovician Decorah Formation, Upper Mississippi Valley. *GSA Special Paper* **306,** 67–86.

Marshall J. D. and Middleton J. D. (1990) Changes in marine isotopic composition and the late Ordovician glaciation. *J. Geol. Soc. (London)* **147,** 1–4.

Marshall J. D., Brenchley P. J., Mason P., Wolff G. A., Astini R. A., Hints L., and Meidla T. (1997) Global carbon isotopic events associated with mass extinction and glaciation in the late Ordovician. *Palaeogeog. Palaeoclimat. Palaeoecol.* **132,** 195–210.

McArthur J. M. (1994) Recent trends in strontium isotope stratigraphy. *Terra Nova* **6,** 331–358.

Middleton P. D., Marshall J. D., and Brenchley P. J. (1991) Evidence for isotopic changes associated with Late Ordovician glaciation from brachiopods and marine cements of central Sweden. *Geol. Surv. Canada Paper* **90-9,** 313–321.

Mii H. S. and Grossman E. L. (1994) Late Pennsylvanian seasonality reflected in the ^{18}O and elemental composition of the brachiopod shell. *Geology* **22,** 661–664.

Mii H. S., Grossmann E. L., Yancey T. E., Chuvashov B., and Egarov A. (2001) Isotopic records of brachiopod shells from the Russian Platform—evidence for the onset of mid-Carboniferous glaciation. *Chem. Geol.* **175,** 133–147.

Milliman J. D. (1974) *Marine Carbonates*, Springer-Verlag, New York. p. 375.

Montañez I. P., Banner J. L., Osleger D. A., Borg L. E., and Bosserman P. J. (1996) Integrated Sr isotope variations and sea-level history of Middle to Upper Cambrian platform carbonates: Implications for the evolution of Cambrian seawater $^{87}Sr/^{86}Sr$. *Geology* **24,** 917–920.

Montañez I. P., Osleger D. A., Banner J. L., Mack L. E., and Musgrove M. (2000) Evolution of the Sr and C isotope composition of Cambrian oceans. *GSA Today* **10,** 1–10.

Morrison O. J. and Brand U. (1986) Palaeoscene No. 5: Geochemistry of recent marine invertebrates. *Geoscience Canada* **13,** 237–254.

Muehlenbacks K. and Clayton R. N. (1976) Oxygen isotope composition of the oceanic crust and its bearing on seawater. *J. Geophys. Res.* **81,** 4365–4369.

Muehlenbachs K. (1998) The oxygen isotopic composition of the oceans, sediments and the seafloor. *Chem. Geol.* **145,** 263–273.

Nikitin I. F., Frid N. M., and Zvontsov V. S. 1990 Paleogeography and main features of volcanicity in the Ordovician of Kazakhstan and North Tien Shan. In *Advances in Ordovician Geology* (eds. C. R. Barnes and S. H. Williams), Geological Survey of Canada, Paper **90–9,** pp. 259–270.

Pancost R. D., Freeman K. H., and Patzowsky M. E. (1999) Organic-matter source variation and the expression of a late Middle Ordovician carbon isotope excursion. *Geology* **27,** 1015–1018.

Patzkowsky M. E., Slupik L. M., Arthur M. A., Pancost R. D., and Freeman K. H. (1997) Late Middle Ordovician environmental change and extinction: Harbinger of the Late Ordovician or continuation of Cambrian patterns. *Geology* **25,** 911–914.

Peterman Z. E., Hedge C. E., and Tourtelot H. A. (1970) Isotopic composition of strontium in seawater throughout Phanerozoic time. *Geochim. Cosmochim. Acta* **34,** 105–120.

Popp B. N., Anderson T. F., and Sanders P. A. (1986) Brachiopods as indicators of original isotopic composition in some Paleozoic limestones. *GSA Bulletin* **97,** 1262–1269.

Qing H. and Veizer J. (1994) Oxygen and carbon isotopic composition of Ordovician brachiopods: Implications for coeval seawater. *Geochim. Cosmochim. Acta* **58,** 4429–4442.

Qing H., Barnes C. R., Buhl D., and Veizer J. (1998) The strontium isotopic composition of Ordovician and Silurian brachiopods and conodonts: Relationships to geological events and implications for coeval seawater. *Geochim. Cosmochim. Acta* **62,** 1721–1733.

Richter F. M., Rowley D. B., and DePaolo D. J. (1992) Sr isotope evolution of seawater: The role of tectonics. *Earth Planet. Sci. Lett.* **109,** 11–23.

Ripperdan R. and Miller J. F. (1995) Carbon isotope ratios from the Cambrian-Ordovician boundary section at Lawson Cove, Ibex Area, Utah. In *Ordovician Odyssey: Short Papers for the Seventh International Symposium on the Ordovician System* (eds. J. D. Cooper, M. L. Droser, and S. C. Finney), pp. 129-132. Pacific Section for Sedimentary Geology (SEPM).

Ripperdan R. L., Magaritz M., and Kirschvink J. L. (1993) Carbon isotope and magnetic polarity evidence for non-depositional events within the Cambrian-Ordovician boundary section near Dayangcha, Jilin Province, China. Geol. Mag. **130,** 443–452.

Ripperdan R. L., Margaritz M., Nicoll R. S., and Shergold J. H. (1992) Simultaneous changes in carbon isotopes, sea level, and conodont biozones within the Cambrian-Ordovician boundary interval at Black Mountain, Australia. *Geology* **20,** 1039–1042.

Ronov A. B., Khain V. E., Balukhovsky A. N., and Seslavinsky K. B. (1980) Quantitative analysis of Phanerozoic sedimentation. *Sediment. Geol.* **25,** 311–325.

Ross J. R. and Ross C. A. (1992) Ordovician sea-level fluctuations. In *Global Perspectives in Ordovician Geology* (eds. B. D. Webby and J. R. Laurie), pp. 327-335. Balkema; Rotterdam.

Ruppel S. C., James E. W., Barrick J. E., Nowlan G., and Uyeno T. T. (1996) High-resolution $^{87}Sr/^{86}Sr$ chemostratigraphy of the Silurian: Implications for event correlation and strontium flux. *Geology* **24,** 831–834.

Schmidt G. A. (l999) Forward modeling of carbonate proxy data from planktonic foraminifera using oxygen isotope tracers in a global ocean model. *Paleoceanography* **14,** 482–497.

Scotese C. R. and McKerrow W. S. (1991) Ordovician plate tectonic reconstructions. *Geological Survey of Canada Paper* **90-9,** 271–282.

Smalley P. C., Higgins A. C., Howarth R. K., Nicholson H., Jones C. E., Swinburne N. H. M., and Bessa J. (1994) Marine strontium isotopes: A Phanerozoic seawater curve for practical sediment dating and correlation. *Geology* **22,** 431–434.

Stein C. A., Stein S., and Pelayo A. M. (1995) Heat flow and hydrothermal circulation. In *Seafloor Hydrothermal Systems: Physical, Chemical, Biological, and Geological Interactions* (eds. S. E. Humphris, R. A. Zierenberg, L. S. Mullineaux, and R. E. Thomson), pp. 425-445. Geophysical Monograph 9, American Geophysical Union.

Stille P., and Shields G. A. (1997) Radiogenic isotope geochemistry of sedimentary and aquatic systems. *Lecture Notes in Earth Science* **68,** Springer Verlag, 217 p.

Tobin K. J. and Walker K. R. (1996) Ordovician low-to-intermediate Mg calcite from Sweden: An example of marine stabilization and implications for Ordovician stable C-O marine isotopes. *Sedimentology* **43,** 719–735.

Tobin K. J., Walker K. R., Steinhauff D. M., and Mora C. I. (1996) Fibrous calcite from the Ordovician of Tennessee: Preservation of marine oxygen isotopic composition and its implications. *Sedimentology* **43,** 235–251.

Underwood C. J., Crowley S. F., Marshall J. D., and Brenchley P. J. (1997) High-resolution carbon isotope stratigraphy of the basal Silurian stratotype (Dob's Linn, Scotland) and its global correlation. *J. Geol. Soc. (London)* **154,** 709–718.

Veizer J. (1989) Strontium isotopes in seawater through time. *Ann. Rev. Earth Planet. Sci.* **17,** 141–167.

Veizer J. and Compston W. (1974) $^{87}Sr/^{86}Sr$ composition of seawater during the Phanerozoic. *Geochim. Cosmochim. Acta* **38,** 1461–1484.

Veizer J., Holser W. T., and Wilgus C. K. (1980) Correlation of $^{13}C/^{12}C$ and $^{34}S/^{32}S$ secular variations. *Geochim. Cosmochim. Acta* **44,** 579–587.

Veizer J., Fritz P., and Jones B. (1986) Geochemistry of brachiopods: Oxygen and carbon isotopic records of Paleozoic oceans. *Geochim. Cosmochim. Acta* **50,** 1679–1696.

Veizer J., Bruckschen P., Pawellek F., Diener A., Podlaha O. G., Carden G. A. F., Jasper T., Korte C., Strauss H., Azmy K., and Ala D. (1997) Oxygen isotope evolution of Phanerozoic seawater. *Palaeogeog. Palaeoclimat. Palaeoecol.* **132,** 159–172.

Veizer J., Ala D., Azmy K., Bruckschen P., Buhl D., Bruhn F., Carden G. A. F., Diener A., Ebneth S., Godderis Y., Jasper T., Korte C.,

Pawellek F., Podlaha O., and Strauss H. (1999) $^{87}Sr/^{86}Sr$, $\delta^{13}C$ and $\delta^{18}O$ evolution of Phanerozoic seawater. *Chem. Geol.* **161,** 59–88.

Veizer J., Goddéris Y.-F., and François L. M. (2000) Evidence for decoupling of atmospheric CO_2 and global climate during the Phanerozoic eon. *Nature* **408,** 698–701.

Wadleigh M. A. and Veizer J. (1992) $^{18}O/^{16}O$ and $^{13}C/^{12}C$ in Lower Ordovician articulate brachiopods: Implication for the isotopic composition of seawater. *Geochim. Cosmochim. Acta* **56,** 431–443.

Wallmann K. (2001) The geological water cycle and the evolution of marine $\delta^{18}O$ values. *Geochim. Cosmochim. Acta* **65,** 2469–2485.

Walker J. G. C. and Lohmann K. C. (1989) Why the oxygen isotopic composition of seawater changes with time. *Geophys. Res. Letts.* **16,** 323–326.

Wang K., Orth C. J., Attrep M. Jr., Chatterton B. D. E., Wang X., and Li J. (1993) The great latest Ordovician extinction on the South China Plate: Chemostratigraphic studies of the Ordovician-Silurian boundary interval on the Yangtze Platform. *Palaeogeog. Palaeoclimat. Palaeoecol.* **104,** 61–79.

Wang K., Chatterton B. D. E., and Wang Y. (1997) An organic carbon isotope record of Late Ordovician to Early Silurian marine sedimentary rocks, Yangtze Sea, South China: Implications for CO2 changes during the Hirnantian glaciation.. *Palaeogeogr., Palaeoclimatol., Palaecol.* **147,** 147–158.

Webby B. D. (1998) Steps toward a global standard for Ordovician stratigraphy. *Newsl. Stratigr.* **36,** 1–33.

Wickman F. E. (1948) Isotope ratios: A clue to the age of certain marine sediments. *J. Geol.* **56,** 61–66.

Wright C. A., Barnes C. R., and Jacobsen S. B. (2002) Neodymium isotopic composition of Ordivician conodonts as a seawater proxy: Testing paleography. *Geochem. Geophys. Geosyst.* **3**(2), 101029/2001GC000195.

Appendix A1. Isotopic, geochemical

Sample	Material	Unit	Location	Series	Stage	T/S	$^{87}Sr/^{86}Sr$	$\delta^{13}C$	$\delta^{18}O$	Mn/Sr	Mg ppm	Fe ppm	Mn ppm	Sr ppm
A61	indeterminate	Bescie	Québec	Lower Silurian	Llandoverian	1	0.707929	0.35	−3.56	0.06	4849	1119	80	1416
Ch14	Dalmanella testudinaria	Kuanyinchiao	South China	Upper Ordovician	“Ashgillian”	6c	0.708308			1.47	3269	2115	1132	769
Ch18	Dalmanella testudinaria	Kuanyinochiao	South China	Upper Ordovician	“Ashgillian”	6c	0.708125			0.42	3881	881	445	1067
Ch20	Plectothyrella crassicosta	Kuanyinchiao	South China	Upper Ordovician	“Ashgillian”	6c	0.708267	5.1	−3.61	0.08	1279	182	87	1157
Ch21	Hindella crassa incipiens	Kuanyinchiao	South China	Upper Ordovician	“Ashgillian”	6c	0.708554	4.17	−3.15	0.03	956	121	26	1012
Ch23	Hindella crassa incipiens	Kuanyinchiao	South China	Upper Ordovician	“Ashgillian”	6c	0.708023	5.83	0.15	0.13	1185	145	160	1236
Ch24	Hindella crassa incipiens	Kuanyinchiao	South China	Upper Ordovician	“Ashgillian”	6c		3.66	−4.13	0.12	1271	488	96	794
Ch25	Hindella crassa incipiens	Kuanyinchiao	South China	Upper Ordovician	“Ashgillian”	6c		5.12	−1.31	0.28	1180	217	317	1124
A56	indeterminate	Laframboise	Québec	Upper Ordovician	“Ashgillian”	6c	0.707923	3.71	−2.09	0.16	10570	1978	163	996
A59	Ancillotoechia fringilla	Laframboise	Québec	Upper Ordovician	“Ashgillian”	6c	0.707907	2.95	−3.19	0.09	5404	1477	83	937
A53	Hesperorthis	Laframboise	Québec	Upper Ordovician	“Ashgillian”	6c	0.707890	3.3	−3.93	0.05	5644	673	58	1210
A52	indeterminate	Lousy cove	Québec	Upper Ordovician	“Ashgillian”	6c	0.707901	0.32	−3.83					
A37	Vellamo	Lousy cove	Québec	Upper Ordovician	“Ashgillian”	6c		0.49	−3.40	0.03	4765	262	44	1280
A48	Clitambonitacea?	Lousy cove	Québec	Upper Ordovician	“Ashgillian”	6c	0.707891	0.2	−3.55	0.04	5093	803	45	1154
A47	indeterminate	Lousy cove	Québec	Upper Ordovician	“Ashgillian”	6c		0.26	−3.47	0.17	6684	1527	168	974
A43	indeterminate	Lousy cove	Québec	Upper Ordovician	“Ashgillian”	6c		0.36	−3.35					
A45	Clitambonitacea?	Lousy cove	Québec	Upper Ordovician	“Ashgillian”	6c		0.69	−3.23	0.29	5737	3777	291	1015
		Prinsta	Québec	Upper Ordovician	“Ashgillian”	6c	0.707874	0.63	−4.20	0.13	5209	1701	202	1513
		Prinsta	Québec	Upper Ordovician	“Ashgillian”	6c		0.89	−3.86	0.08	5244	1807	97	1240
A35	Parastrophinella	Prinsta	Québec	Upper Ordovician	“Ashgillian”	6c	0.707896	0.63	−2.92	0.02	4150	561	28	1294
		Prinsta	Québec	Upper Ordovician	“Ashgillian”	6c	0.707887	0.32	−3.68					
		Prinsta	Québec	Upper Ordovician	“Ashgillian”	6c		0.24	−3.40	0.09	8168	1534	104	1215
		Prinsta	Québec	Upper Ordovician	“Ashgillian”	6c	0.707887	0.39	−3.53	0.16	8666	4746	152	929
		Velleda	Québec	Upper Ordovician	“Ashgillian”	6c		0.24	−3.35	0.12	5365	1377	143	1206
		Velleda	Québec	Upper Ordovician	“Ashgillian”	6c	0.707888	0.73	−3.13	0.07	6747	1732	88	1235
		Velleda	Québec	Upper Ordovician	“Ashgillian”	6c	0.708065	0.58	−4.31	0.10	5186	1152	154	1553
		Velleda	Québec	Upper Ordovician	“Ashgillian”	6c	0.707897	0.41	−3.87	0.11	5542	2088	124	1155
		Velleda	Québec	Upper Ordovician	“Ashgillian”	6c		0.6	−3.52	0.16	7111	1527	210	1338
		Velleda	Québec	Upper Ordovician	“Ashgillian”	6c		0.97	−2.76	0.25	4378	568	192	780
		Velleda	Québec	Upper Ordovician	“Ashgillian”	6c	0.707856	0.55	−3.43	0.20	8300	3800	193	972
		Velleda	Québec	Upper Ordovician	“Ashgillian”	6c		1.04	−2.78					
		Velleda	Québec	Upper Ordovician	“Ashgillian”	6c	0.707903	1.26	−2.89	0.11	4450	318	124	1080
A28	Ancillotoechia fringilla	Velleda	Québec	Upper Ordovician	“Ashgillian”	6c	0.707876	1.72	−3.15	0.21	4031	625	208	984
A29	indeterminate	Velleda	Québec	Upper Ordovician	“Ashgillian”	6c		1.1	−3.27	0.07	4810	1145	78	1187
A34	indeterminate	Velleda	Québec	Upper Ordovician	“Ashgillian”	6c		0.89	−3.74	0.19	7129	2217	235	1239
Ch13a	Altaethyrella zhejiangensis	Xiazhen	South China	Upper Ordovician	“Ashgillian”	6b	0.707867	0.315	−5.74	0.14	1254	273	74	538
Ch26	Altaethyrella zhejiangensis	Xiazhen	South China	Upper Ordovician	“Ashgillian”	6b	0.707982	0.12	−6.95	0.17	2434	1058	123	711
Ch27	Altaethyrella zhejiangensis	Xiazhen	South China	Upper Ordovician	“Ashgillian”	6b		0.45	−6.53	0.18	1996	1403	125	703
Ch28	Altaethyrella zhejiangensis	Xiazhen	South China	Upper Ordovician	“Ashgillian”	6b		0.21	−6.90	0.12	1625	991	83	703
Ch29	Altaethyrella zhejiangensis	Xiazhen	South China	Upper Ordovician	“Ashgillian”	6b	0.707905	0.21	−6.89	0.09	2345	354	73	806
Ch30	Altaethyrella zhejiangensis	Xiazhen	South China	Upper Ordovician	“Ashgillian”	6b		0.28	−6.92	0.15	2689	1030	106	717
Ch31	Ovalospira dichotoma	Xiazhen	South China	Upper Ordovician	“Ashgillian”	6b	0.708095			0.29	2313	813	125	438
Ch34	Ovalospira dichotoma	Xiazhen	South China	Upper Ordovician	“Ashgillian”	6b	0.708149							
CN08	Rafinesquina ponderosa	Liberty	Ohio, USA	Upper Ordovician	“Ashgillian”	6b	0.707853	0.01	−4.70					
CN10	Onniella	Waynesville	Ohio, USA	Upper Ordovician	“Ashgillian”	6b	0.707843	−0.35	−4.60					
CN11	Onniella	Waynesville	Ohio, USA	Upper Ordovician	“Ashgillian”	6b		0.15	−4.19					
CN05	Onniella ?multisecta	Waynesville	Ohio, USA	Upper Ordovician	“Ashgillian”	6b	0.707839	0.29	−4.23					
CN06	Hebertella	Waynesville	Ohio, USA	Upper Ordovician	“Ashgillian”	6b		0.51	−4.20					

(continued)

Appendix A1. (Continued)

Sample	Material	Unit	Location	Series	Stage	T/S	$^{87}Sr/^{86}Sr$	$\delta^{13}C$	$\delta^{18}O$	Mn/Sr	Mg ppm	Fe ppm	Mn ppm	Sr ppm
CN07	Leptaena	Waynesville	Ohio, USA	Upper Ordovician	"Ashgillian"	6b		−0.06	−4.52					
CN01	Onniella	Arnheim	Ohio, USA	Upper Ordovician	"Ashgillian"	6b	0.707854	0.54	−3.71					
CN02	Onniella	Arnheim	Ohio, USA	Upper Ordovician	"Ashgillian"	6b	0.707878	0.11	−4.21					
CN03	Onniella	Arnheim	Ohio, USA	Upper Ordovician	"Ashgillian"	6b		0.31	−4.10					
CN04	Rafinesquina ponderasa	Arnheim	Ohio, USA	Upper Ordovician	"Ashgillian"	6b	0.707852	−0.3	−4.27					
CN15	Dalmanella	Fairview	Ohio, USA	Upper Ordovician	"Ashgillian"	5d	0.707895	−0.07	−3.95					
CN17	Dalmanella	Fairview	Ohio, USA	Upper Ordovician	"Ashgillian"	5d	0.707907	−0.69	−3.82					
CN18	Hebertella	Fairview	Ohio, USA	Upper Ordovician	"Ashgillian"	5d	0.707845	1.34	−3.53					
CN19	Platystrophia	Fairview	Ohio, USA	Upper Ordovician	"Ashgillian"	5d		−0.02	−5.13					
CN20	Platystrophia	Corriville	Ohio, USA	Upper Ordovician	"Ashgillian"	5d	0.707895	0.56	−5.36					
CN21	indeterminate	Corriville	Ohio, USA	Upper Ordovician	"Ashgillian"	5d	0.707873	−0.27	−5.19					
CN22	Platystrophia	Bell View	Ohio, USA	Upper Ordovician	"Ashgillian"	5d	0.707876	−0.01	−5.54					
CN23	Rafinesquina?	Bell View	Ohio, USA	Upper Ordovician	"Ashgillian"	5d		0.55	−5.01					
CN14	Dalmanella	Kope	Ohio, USA	Upper Ordovician	"Ashgillian"	5d	0.707890	−0.49	−5.50					
CN12	Dalmanella?	Kope	Ohio, USA	Upper Ordovician	"Caradocian"	5c	0.707908							
CN13	Eoplectodonta	Kope	Ohio, USA	Upper Ordovician	"Caradocian"	5c	0.707949	−2.07	−6.52					
MO01	indeterminate	Kings Lake	Missouri, USA	Upper Ordovician	"Caradocian"	5b	0.708033	0.33	−6.00	0.03	1546	2088	26	876
MO02	indeterminate	Spechts Ferry	Missouri, USA	Upper Ordovician	"Caradocian"	5b	0.708055	−0.57	−5.14	0.27	2031	282	258	944
MO03	indeterminate	Spechts Ferry	Missouri, USA	Upper Ordovician	"Caradocian"	5b		−1.74	−6.82	0.02	2131	1598	41	2541
MO05	indeterminate	Spechts Ferry	Missouri, USA	Upper Ordovician	"Caradocian"	5b	0.708050							
MO06	indeterminate	Spechts Ferry	Missouri, USA	Upper Ordovician	"Caradocian"	5b		−0.51	−5.21	0.32	900	312	138	431
MO07	Pionodema	Spechts Ferry	Missouri, USA	Upper Ordovician	"Caradocian"	5b		1.55	−5.26	0.01	1831	186	11	1963
MO08	indeterminate orthid	Spechts Ferry	Missouri, USA	Upper Ordovician	"Caradocian"	5b	0.708126	−1.18	−6.18		1293	172		
MO09	indeterminate	Spechts Ferry	Missouri, USA	Upper Ordovician	"Caradocian"	5b		−0.69	−6.21	0.01	1383	241	13	1383
MO10	Pionodema	Spechts Ferry	Missouri, USA	Upper Ordovician	"Caradocian"	5b	0.708068				1058	288		1058
MO11	Rhynchonellid	Spechts Ferry	Missouri, USA	Upper Ordovician	"Caradocian"	5b		−0.47	−5.19		1620	b.d.l.		1620
MO13	Pionodema	Kings Lake	Missouri, USA	Upper Ordovician	"Caradocian"	5b	0.708072	0.01	−6.60	0.09	145	51	13	145
MO14	Pionodema	Kings Lake	Missouri, USA	Upper Ordovician	"Caradocian"	5b		0.3	−5.53	0.03	362	631	12	362
MO17	Dalmanella?	Bloomsdale	Missouri, USA	Upper Ordovician	"Caradocian"	5b	0.708187	−1.24	−5.08					
MO18	Dalmanella?	Bloomsdale	Missouri, USA	Upper Ordovician	"Caradocian"	5b	0.708190	−1.52	−5.15					
MO19	Dalmanella?	Bloomsdale	Missouri, USA	Upper Ordovician	"Caradocian"	5b		−1.19	−4.19					
MO20	Dalmanella?	Bloomsdale	Missouri, USA	Upper Ordovician	"Caradocian"	5b	0.708202							
KY01	Onniella?	Tyrone	Kentucky, USA	Upper Ordovician	"Caradocian"	5b	0.707987	0.62	−5.76	0.26	2603	2155	207	810
KY02	Onniella?	Tyrone	Kentucky, USA	Upper Ordovician	"Caradocian"	5b		0.22	−6.23	0.08	2283	4783	109	1413
KY03	Onniella?	Tyrone	Kentucky, USA	Upper Ordovician	"Caradocian"	5b	0.707961	0.06	−6.46	0.14	2359	13380	282	2007
KY04	indet. Rhynchoncllid	Lexington	Kentucky, USA	Upper Ordovician	"Caradocian"	5b	0.707972	0.52	−6.19	0.21	1012	1071	149	714
KY05	indeterminate	Lexington	Kentucky, USA	Upper Ordovician	"Caradocian"	5b		0.25	−5.43	0.85	1388	319	253	297
KY06	indeterminate orthid.	Lexington	Kentucky, USA	Upper Ordovician	"Caradocian"	5b	0.707980	0.72	−4.36	0.58	3958	1131	327	565
KY07	Hebertella?	Lexington	Kentucky, USA	Upper Ordovician	"Caradocian"	5b	0.707971	0	−6.41	0.20	2265	289	144	722
KY08	Dalmanella?	Lexington	Kentucky, USA	Upper Ordovician	"Caradocian"	5b		1.22	−5.31	0.31	5484	1048	323	1048
KY09	Dalmanella?	Lexington	Kentucky, USA	Upper Ordovician	"Caradocian"	5b	0.707996	0.85	−5.37	0.19	3043	1848	272	1413
KY10	Dalmanella?	Lexington	Kentucky, USA	Upper Ordovician	"Caradocian"	5b		0.48	−6.05	0.15	2890	642	138	940
KY11*	Dalmanella?	Lexington	Kentucky, USA	Upper Ordovician	"Caradocian"	5b	0.708005	1.05	−5.87	0.02	2300	1550	150	605
KY12	indeterminate	Lexington	Kentucky, USA	Upper Ordovician	"Caradocian"	5b	0.708008	0.13	−6.06	0.64	2920	291	474	744
KY13	indeterminate	Lexington	Kentucky, USA	Upper Ordovician	"Caradocian"	5b		−0.11	−5.64	0.34	2852	305	505	1491
KY14	strophomenid	Lexington	Kentucky, USA	Upper Ordovician	"Caradocian"	5b	0.707949			0.65	3416	326	543	839
KY15*	indeterminate orthid.	Lexington	Kentucky, USA	Upper Ordovician	"Caradocian"	5b	0.707962	0.02	−6.01	0.97	2500	257	566	581
LS01	indeterminate	Bobcaygeon	Kentucky, USA	Upper Ordovician	"Caradocian"	5b	0.707846	0.13	−4.57	0.35	2394	842	507	1462

(continued)

Appendix A1. (Continued)

Sample	Material	Unit	Location	Series	Stage	T/S	$^{87}Sr/^{86}Sr$	$\delta^{13}C$	$\delta^{18}O$	Mn/Sr	Mg ppm	Fe ppm	Mn ppm	Sr ppm
LS05	indeterminate	Bobcaygeon	Kentucky, USA	Upper Ordovician	"Caradocian"	5b	0.708009	1.19	−4.92	0.08	2727	727	91	1091
LS02	indeterminate	Gull River	Kentucky, USA	Upper Ordovician	"Caradocian"	5b	0.708107	−1.19	−4.95	0.52	2924	280	333	636
LS04	indeterminate	Gull River	Kentucky, USA	Upper Ordovician	"Caradocian"	5b	0.708095	−0.93	−4.96	0.52	2745	708	454	875
OK01	Mimella extens	Bromide	Oklahoma, USA	Upper Ordovician	"Caradocian"	5b	0.708365	−0.804	−6.22	0.04	3035	134	39	878
OK02	Mimella extensa	Bromide	Oklahoma, USA	Upper Ordovician	"Caradocian"	5b		−1.1	−6.02	0.05	3134	247	46	900
OK03	Mimella extensa	Bromide	Oklahoma, USA	Upper Ordovician	"Caradocian"	5b	0.708366	−1.19	−5.63	0.08	3090	342	64	833
OK04	Mimella extensa	Bromide	Oklahoma, USA	Upper Ordovician	"Caradocian"	5b		−1.29	−5.23	0.01	2557	402	10	915
OK05	Mimella extensa	Bromide	Oklahoma, USA	Upper Ordovician	"Caradocian"	5b	0.708158	−0.113	−4.60		2590	107		905
OK06	Mimella extensa	Bromide	Oklahoma, USA	Upper Ordovician	"Caradocian"	5b	0.708158	0.139	−3.96		3051	246		876
OK07	Leptaena?	Bromide	Oklahoma, USA	Upper Ordovician	"Caradocian"	5b		−0.908	−6.21		2136	217		1011
OK08	Mimella extensa	Bromide	Oklahoma, USA	Upper Ordovician	"Caradocian"	5b		−0.286	−4.75		2964	57		935
OK09	Leptaena?	Bromide	Oklahoma, USA	Upper Ordovician	"Caradocian"	5b		−0.503	−4.18	0.07	2616	233	44	610
OK10	Mimella extensa	Bromide	Oklahoma, USA	Upper Ordovician	"Caradocian"	5b	0.708155	−1.096	−5.34	0.02	3345	106	15	878
OK11	Mimella extensa	Bromide	Oklahoma, USA	Upper Ordovician	"Caradocian"	5b		−0.39	−5.25	0.02	3201	85	17	971
OK17	indeterminate	Bromide	Oklahoma, USA	Upper Ordovician	"Caradocian"	5b	0.708150	−0.69	−5.09	0.05	3352	175	45	866
OK18	indeterminate	Bromide	Oklahoma, USA	Upper Ordovician	"Caradocian"	5b	0.708159			0.01	2303	418	12	1323
OK20	indeterminate orthid	McLish	Oklahoma, USA	Middle Ordovician	Darriwilian	4c	0.708602	−0.62	−6.48		4255	1250		2500
OK21	indeterminate orthid	McLish	Oklahoma, USA	Middle Ordovician	Darriwilian	4c	0.708650	−0.38	−6.21	0.18	3140	694	247	1384
OK12	indeterminate	McLish	Oklahoma, USA	Middle Ordovician	Darriwilian	4b	0.708707	−1.87	−5.54	0.47	2259	475	434	916
OK14	indeterminate	McLish	Oklahoma, USA	Middle Ordovician	Darriwilian	4b	0.708696	−1.54	−5.60	0.44	2684	685	458	1052
OK15	indeterminate	McLish	Oklahoma, USA	Middle Ordovician	Darriwilian	4b	0.708696	−1.68	−5.66	0.24	2246	326	264	1092
OK16	indeterminate	McLish	Oklahoma, USA	Middle Ordovician	Darriwilian	4b		−1.74	−6.65	0.33	1807	453	363	1108
Ch36	Leptellina sp.	Shihtzepu	South China	Middle Ordovician	Darriwilian	4b	0.708838	0.94	−7.61					
Ch39	Leptellina sp.	Shihtzepu	South China	Middle Ordovician	Darriwilian	4b	0.708796	1.82	−7.76					
OK19	indeterminate	Oil Creek	Oklahoma, USA	Middle Ordovician	Darriwilian	4a		−1.51	−7.02	0.07	2952	924	136	1858
OK22	Multicostella convexa	Oil Creek	Oklahoma, USA	Middle Ordovician	Darriwilian	4a	0.708788	−1.99	−6.46	0.15	1985	838	265	1757
OK23	Multicostella convexa	Oil Creek	Oklahoma, USA	Middle Ordovician	Darriwilian	4a		−1.81	−6.08	0.17	2688	1143	304	1777
OK24	indeterminate	Oil Creek	Oklahoma, USA	Middle Ordovician	Darriwilian	4a	0.708742	−1.94	−5.45	0.16	3432	1376	355	2175
OK25	Hindella-like smooth shell	Oil Creek	Oklahoma, USA	Middle Ordovician	Darriwilian	4a	0.708740	−2.1	−6.05	0.23	3703	1375	516	2250
OK26	Hindella-like smooth shell	Oil Creek	Oklahoma, USA	Middle Ordovician	Darriwilian	4a		−2	−5.96	0.14	2673	1019	364	2519
OK27	indeterminate	Oil Creek	Oklahoma, USA	Middle Ordovician	Darriwilian	4a		−2.53	−6.48	0.04	2865	1117	426	1023
Ch42	Yangtzeella polol	Dawan	South China	Middle Ordovician	Darriwilian	4a	0.708760	−0.44	−5.54					
Ch43	Yangtzeella polol	Dawan	South China	Middle Ordovician	Darriwilian	4a		−2.02	−6.35					
Ch44	Yangtzeella polol	Dawan	South China	Middle Ordovician	Darriwilian	4a		−1.93	−7.36					
Ch45	Pseudomimella formosa	Dawan	South China	Middle Ordovician	Darriwilian	4a	0.708757							
Ch46	Pseudomimella formosa	Dawan	South China	Middle Ordovician	Darriwilian	4a		−0.77	−6.17					
Ch47	Pseudomimella formosa	Dawan	South China	Middle Ordovician	Darriwilian	4a	0.708744	−0.56	−6.73					
Ch48	Nereidella sinuata	Dawan	South China	Middle Ordovician	Darriwilian	4a	0.708731	−0.8	−6.77					
Ch49	Nereidella sinuata	Dawan	South China	Middle Ordovician	Darriwilian	4a		−0.89	−6.98					
Ch50	Nereidella sinuata	Dawan	South China	Middle Ordovician	Darriwilian	4a		−0.55	−6.41					
Ch51	ereidella sinuata	Dawan	South China	Middle Ordovician	Darriwilian	4a		−0.82	−6.56					
Ch52	Martellia ichangenala	Dawan	South China	Middle Ordovician	Darriwilian	4a	0.708738	−2.26	−7.31					
Ch53	Martellia ichangenala	Dawan	South China	Middle Ordovician	Darriwilian	4a		−0.6	−7.50					
Ch54	Martellia ichangenala	Dawan	South China	Middle Ordovician	Darriwilian	4a	0.708732	−1.18	−7.72					
Ch55	Martellia ichangenala	Dawan	South China	Middle Ordovician	Darriwilian	4a		−0.99	−8.05					
Csp01*	indeterminate	Volkhov	Russia	Middle Ordovician	"Stage 3"	3a/3b	0.708747	−0.521	−6.33	0.25	2750		251	1008
Csp02b	indeterminate	Volkhov	Russia	Middle Ordovician	"Stage 3"	3a/3b		0.323	−5.57	0.31	4641		288	925
Csp03	Antigonambonites planus	Volkhov	Russia	Middle Ordovician	"Stage 3"	3a/3b	0.708749	−0.219	−5.94	0.20	4408		216	1087
Csp04	Productus obtusa	Volkhov	Russia	Middle Ordovician	"Stage 3"	3a/3b		−0.303	−5.85					

(continued)

Appendix A1. (Continued)

Sample	Material	Unit	Location	Series	Stage	T/S	$^{87}Sr/^{86}Sr$	$\delta^{13}C$	$\delta^{18}O$	Mn/Sr	Mg ppm	Fe ppm	Mn ppm	Sr ppm
Csp06a	Antigonambonites planus	Volkhov	Russia	Middle Ordovician	"Stage 3"	3a/3b		−0.309	−5.89	0.19	2382		224	1201
Csp07a	indeterminate	Volkhov	Russia	Middle Ordovician	"Stage 3"	3a/3b	0.708714	−0.571	−6.06	0.41	4577		362	882
Csp08b	Antigonambonites planus	Volkhov	Russia	Middle Ordovician	"Stage 3"	3a/3b		−0.054	−5.88	0.49	5928		424	868
Csp09b	Antigonambonites planus	Volkhov	Russia	Middle Ordovician	"Stage 3"	3a/3b		−0.524	−5.69	0.74	5590	1814	665	896
Csp10b	Antigonambonites planus	Volkhov	Russia	Middle Ordovician	"Stage 3"	3a/3b	0.708756	−0.374	−5.88	0.43	5706	1741	444	1032
Csp11b	indeterminate	Volkhov	Russia	Middle Ordovician	"Stage 3"	3a/3b		−0.621	−5.44	0.17	2625	777	205	1214
Csp05a	Billingenium	Leetse	Russia	Middle Ordovician	"Stage 3"	3a/3b	0.708810	−0.668	−5.86	0.33	5152		324	976
Ch02a	Pseudomimella formosa	Dawan	South China	Middle Ordovician	"Stage 3"	3a	0.708741			0.31	2538	470	322	1047
Ch03a	Pseudomimella formosa	Dawan	South China	Middle Ordovician	"Stage 3"	3a		−2.367	−7.01	0.20	2086	325	177	883
Ch04a	Martellia ichangenala	Dawan	South China	Middle Ordovician	"Stage 3"	3a	0.708736			0.02	2434	929	22	1150
Ch05a	Martellia ichangenala	Dawan	South China	Middle Ordovician	"Stage 3"	3a		−0.856	−7.43	0.14	2959	475	190	1345
Ch06a	Martellia ichangenala	Dawan	South China	Middle Ordovician	"Stage 3"	3a		−1.502	−7.74	0.06	2716	138	82	1302
Ch07a	Nereidella sinuata	Dawan	South China	Middle Ordovician	"Stage 3"	3a	0.708753	−1.264	−6.67	0.50	4358	1323	499	990
Ch08a	Nereidella sinuata	Dawan	South China	Middle Ordovician	"Stage 3"	3a		−1.344	−6.88	0.24	3235	405	228	946
Ch10a	Yangtzeella polol	Dawan	South China	Middle Ordovician	"Stage 3"	3a	0.708733	−2.195	−7.03	0.15	3267	446	136	879
Ch11a	Yangtzeella polol	Dawan	South China	Middle Ordovician	"Stage 3"	3a		−1.632	−6.30	0.15	4128	315	171	1153
Ch12a	Yangtzeella polol	Dawan	South China	Middle Ordovician	"Stage 3"	3a		−1.5	−6.51	0.52	4473	1025	552	1066
BAu01	Aporthophyla	Horn Valley	Australia	Middle Ordovician	"Stage 3"	3a	0.708870	−1.952	−7.56	0.62	5111		487	781
BAu02	Aporthophyla	Horn Valley	Australia	Middle Ordovician	"Stage 3"	3a	0.708777							
BAu03	Aporthophyla	Horn Valley	Australia	Middle Ordovician	"Stage 3"	3a	0.708810	−1.32	−7.60	0.22	3345		258	1185
BAu04	Aporthophyla	Horn Valley	Australia	Middle Ordovician	"Stage 3"	3a	0.708772	−1.265	−7.39	0.14	3838		168	1168
BAu05	Aporthophyla	Horn Valley	Australia	Middle Ordovician	"Stage 3"	3a		−1.54	−7.34	0.65	3796		702	1088
BAu06	Aporthophyla	Horn Valley	Australia	Middle Ordovician	"Stage 3"	3a		−1.46	−7.43	0.83	3367		930	1121
BAu07	Aporthophyla	Horn Valley	Australia	Middle Ordovician	"Stage 3"	3a		−1.829	−7.15	9.49	4415		2125	224
BAu08	Aporthophyla	Horn Valley	Australia	Middle Ordovician	"Stage 3"	3a	0.708795	−1.17	−7.44	0.27	2778		320	1169
BAu09	Aporthophyla	Horn Valley	Australia	Middle Ordovician	"Stage 3"	3a		−1.444	−7.11	2.23	3497		1694	760
BAu10	Aporthophyla	Horn Valley	Australia	Middle Ordovician	"Stage 3"	3a	0.708750	−1.261	−7.56	0.56	3280		426	780
BAu11	Aporthophyla	Horn Valley	Australia	Middle Ordovician	"Stage 3"	3a		−1.305	−7.29	0.22	2286		274	1221
BAu12	Aporthophyla	Horn Valley	Australia	Middle Ordovician	"Stage 3"	3a		−1.192	−7.20	0.32	3543		342	1055
BAu13	Aporthophyla	Horn Valley	Australia	Middle Ordovician	"Stage 3"	3a		−1.092	−6.77	0.68	2421		847	1240
BAu14	Aporthophyla	Horn Valley	Australia	Middle Ordovician	"Stage 3"	3a		−1.063	−7.25	1.02	2378		268	264
Alb01	Orthambonites	L. Kanosh Shale	Utah, USA	Middle Ordovician	"Stage 3"	3a	0.709371	−2.894	−8.55	0.66	4529		453	689
Alb02b	Orthambonites	L. Olive Shale	Utah, USA	Middle Ordovician	"Stage 3"	3a		−2.608	−8.85	0.44	4433		406	932
Alb03b	Orthambonites	L. Olive Shale	Utah, USA	Middle Ordovician	"Stage 3"	3a	0.709514	−2.633	−8.50	0.40	3512		328	814
Alb04b	Orthambonites	L. Olive Shale	Utah, USA	Middle Ordovician	"Stage 3"	3a		−2.415	−9.03	0.50	5812		417	828
Alb05b	Orthambonites	L. Olive Shale	Utah, USA	Middle Ordovician	"Stage 3"	3a	0.709141	−2.975	−8.66	0.76	4377		447	585
Csp12	Ranorthis trivia (Rubel)	Leetse	Russia	Lower Ordovician	"Stage 2"	2c	0.708806							
Csp14	Pandarina tetragona	Leetse	Russia	Lower Ordovician	"Stage 2"	2c	0.708805							
Csp17	Pandarina tetragona	Leetse	Russia	Lower Ordovician	"Stage 2"	2c	0.708801							
Alb06b	Hesperonomiella	m. Simpson Group	Oklahoma, USA	Lower Ordovician	"Stage 2"	2c	0.708878	−1.114	−8.99	0.12	4618		125	1024
Alb07b	Hesperonomiella	Wahwah	Utah, USA	Lower Ordovician	"Stage 2"	2c		−0.899	−8.81	0.10	3769	775	122	1162
Alb08b	Hesperonomiella	Wahwah	Utah, USA	Lower Ordovician	"Stage 2"	2c	0.708930	−1.082	−9.35	0.14	5286	1074	157	1123
Alb09b	Hesperonomiella	Wahwah	Utah, USA	Lower Ordovician	"Stage 2"	2c		−1.1	−8.83	0.12	3774	422	147	1217
Alb10b	Hesperonomiella	Wahwah	Utah, USA	Lower Ordovician	"Stage 2"	2c	0.709132	−1.167	−8.58	0.21	4678	577	208	994
Alb11b	Hesperonomiella	Wahwah	Utah, USA	Lower Ordovician	"Stage 2"	2c		−0.959	−8.76	0.07	4195	334	80	1160
Alb12b	Hesperonomiella	Wahwah	Utah, USA	Lower Ordovician	"Stage 2"	2c		−0.58	−8.21	0.18	3413	1468	119	675
Alb01	Orthambonites	L. Kanosh Shale	Utah, USA	Middle Ordovician	"Stage 3"	3a	0.709371	−2.894	−8.55	0.66	4529		453	689
Alb02b	Orthambonites	L. Olive Shale	Utah, USA	Middle Ordovician	"Stage 3"	3a		−2.608	−8.85	0.44	4433		406	932

(continued)

Appendix A1. (Continued)

Sample	Material	Unit	Location	Series	Stage	T/S	$^{87}Sr/^{86}Sr$	$\delta^{13}C$	$\delta^{18}O$	Mn/Sr	Mg ppm	Fe ppm	Mn ppm	Sr ppm
Alb03b	Orthambonites	L. Olive Shale	Utah, USA	Middle Ordovician	"Stage 3"	3a	0.709514	−2.633	−8.50	0.40	3512		328	814
Alb04b	Orthambonites	L. Olive Shale	Utah, USA	Middle Ordovician	"Stage 3"	3a		−2.415	−9.03	0.50	5812		417	828
Alb05b	Orthambonites	L. Olive Shale	Utah, USA	Middle Ordovician	"Stage 3"	3a	0.709141	−2.975	−8.66	0.76	4377		447	585
Csp12	Ranorthis trivia (Rubel)	Leetse	Russia	Lower Ordovician	"Stage 2"	2c	0.708806							
Csp14	Pandarina tetragona	Leetse	Russia	Lower Ordovician	"Stage 2"	2c	0.708805							
Csp17	Pandarina tetragona	Leetse	Russia	Lower Ordovician	"Stage 2"	2c	0.708801							
Alb06b	Hesperonomiella	m. Simpson Group	Oklahoma, USA	Lower Ordovician	"Stage 2"	2c	0.708878	−1.114	−8.99	0.12	4618		125	1024
Alb07b	Hesperonomiella	Wahwah	Utah, USA	Lower Ordovician	"Stage 2"	2c		−0.899	−8.81	0.10	3769	775	122	1162
Alb08b	Hesperonomiella	Wahwah	Utah, USA	Lower Ordovician	"Stage 2"	2c	0.708930	−1.082	−9.35	0.14	5286	1074	157	1123
Alb09b	Hesperonomiella	Wahwah	Utah, USA	Lower Ordovician	"Stage 2"	2c		−1.1	−8.83	0.12	3774	422	147	1217
Alb10b	Hesperonomiella	Wahwah	Utah, USA	Lower Ordovician	"Stage 2"	2c	0.709132	−1.167	−8.58	0.21	4678	577	208	994
Alb11b	Hesperonomiella	Wahwah	Utah, USA	Lower Ordovician	"Stage 2"	2c		−0.959	−8.76	0.07	4195	334	80	1160
Alb12b	Hesperonomiella	Wahwah	Utah, USA	Lower Ordovician	"Stage 2"	2c		−0.58	−8.21	0.18	3413	1468	119	675
Ch56	Yangtzeella sp.	Meitan	South China	Lower Ordovician	"Stage 2"	2b	0.709103							
Ch58	Sinorthis typica	Meitan	South China	Lower Ordovician	"Stage 2"	2b	0.709106							
Ch59	Sinorthis typica	Meitan	South China	Lower Ordovician	"Stage 2"	2b	0.708957							
Csp24	Prot. ukbalakeria Adr.	?Hunnebergian	Kazakhstan	Lower Ordovician	"Stage 2"	2b	0.708981							
Ch60	Tritoechia sp.	Hunghuayuan	South China	Lower Ordovician	"Stage 2"	2a	0.708937	−1.1	−9.83					
Ch61	Tritoechia sp.	Hunghuayuan	South China	Lower Ordovician	"Stage 2"	2a		−1.14	−11.14					
Ch62	Tritoechia sp.	Hunghuayuan	South China	Lower Ordovician	"Stage 2"	2a		−0.73	−9.97					
Ch63	Orthis sp.	Hunghuayuan	South China	Lower Ordovician	"Stage 2"	2a	0.708930	−0.92	−9.49					
Ch64	Diparelasma	Hunghuayuan	South China	Lower Ordovician	"Stage 2"	2a	0.709120	−1.52	−10.22					
Csp22	Prot. ukbalakeria Adr.	?Hunnerbergian	Kazakhstan	Lower Ordovician	"Stage 2"	2a	0.709076							
Ch19a	Tritoechia sp.	Tungtzu	South China	Lower Ordovician	Tremadocian	1		−0.031	−8.88	28.26	61250	5825	1413	50
Ch20a	Tritoechia sp.	Tungtzu	South China	Lower Ordovician	Tremadocian	1		−0.515	−9.42	3.10	10368	1128	415	134
Ch66	Tritoechia sp.	Tungtzu	South China	Lower Ordovician	Tremadocian	1	0.709034							
Ch67	Tritoechia sp.	Tungtzu	South China	Lower Ordovician	Tremadocian	1	0.709012							
Ch68	Tritoechia sp.	Tungtzu	South China	Lower Ordovician	Tremadocian	1	0.709005	−0.77	−9.07					

T/S = biostratigraphic time slice.